2019

Characterization of the Novel Interaction Between Neisseria gonorrhoeae TdfJ and its Human Ligand S100A7

Stavros Maurakis
Virginia Commonwealth University

CHARACTERIZATION OF THE NOVEL INTERACTION BETWEEN *NEISSERIA GONORRHOEAE* TDFJ AND ITS HUMAN LIGAND S100A7

A Thesis submitted in partial fulfillment of the requirements for the degree of Master of Science at Virginia Commonwealth University.

by

STAVROS ANDREW MAURAKIS
B.S., Virginia Polytechnic Institute and State University, 2014

Director: CYNTHIA NAU CORNELISSEN, PH.D.
PROFESSOR, DEPARTMENT OF MICROBIOLOGY AND IMMUNOLOGY

Virginia Commonwealth University
Richmond, VA
January 2019

Acknowledgements

To begin, I'd like to express my endless gratitude to my mentor, Dr. Cynthia Cornelissen, for welcoming me into her lab and offering unwavering support, thoughtful insight, constructive criticism, and friendship during my graduate career. I will forever be grateful for the opportunity to learn from a scientist who is so intelligent, enthusiastic, and patient; I will carry the lessons I've learned under her tutelage with me for a lifetime. Next, I would like to thank my graduate advisory committee: Dr. Gail Christie and Dr. Todd Kitten. Their guidance, instruction, and support have been instrumental in completion of this degree. I'd also like to thank Dr. Walter Chazin, whose laboratory generously supplied the S100 proteins used in this study.

I'd like to also extend thanks to all those with whom I've shared both happiness and heartache in the lab. To Mike, Julie, Olivia, Ashley, Sandhya, Alexis, and Carlos: You all made my time in the lab so wonderful through your friendship, advice, and compassion. I see us a part of a unique family who all understand the demands of graduate study, and I think we all had to lean on each other from time to time!

Finally, I'd like to extend a few personal thanks to my family and friends. To my amazing fiancée Sara, thank you for always being there to love and support me through all parts of my life while always striving to better yourself. I'll love you always. To my parents, Tim and Jo Ann, thank you for instilling in me the virtues of hard work, integrity, confidence, and so many others. I am so proud to call myself your son. To my older sister Catherine and my brother-in-law Michael, thank you for always being there to offer your love, support, laughs, and perspectives as I grew into adulthood. I've learned more from you both than you could imagine. To all others, of whom there are too many to name, you've been no less important in helping to keep me motivated, grounded, and supported not only through graduate school, but my entire life. You all know who you are, and to you I'm eternally grateful.

Lastly, I'd like to acknowledge my two adorable cats, Shinx and Buffy, who distract me with their silliness and ask me for treats when I'm trying to study. And speaking of distractions, I'd like to mention my FRB teammates. As a lifelong fan of motorsports, sometimes the best way to spend your Sundays is by doing competitive sim racing for several hours instead of working!

Table of Contents

Page

List of Tables

Page

List of Figures

Page

List of Abbreviations

°C	degrees Celsius
AP	alkaline phosphatase
BCA	bicinchoninic acid
BCIP	5-Bromo-4-chloro-3-indolyl phosphate
bp	base pair
BSA	bovine serum albumin
bTf	bovine transferrin
Ca	calcium
CDC	Centers for Disease Control and Prevention
CDM	Chelexed defined media
CFU	colony forming unit
CO_2	carbon dioxide
Cp	Calprotectin
Da	Dalton
DAPI	4’,6-diamidino-2-phenylindole
Dfo	Desferal
DNA	deoxyribonucleic acid

EDTA	Ethylenediaminetetraacetic acid
ELISA	enzyme-linked immunosorbent assay
ECL	enhanced chemiluminescence
Fe	iron
$FeCl_2$	ferrous chloride
$Fe(NO_3)_3$	ferric nitrate
g	gram
GCB	gonococcal medium broth
h	hours
HCl	hydrochloric acid
HEPES	4-(2-hydroxyethyl)-1-piperazineethanesulfonic acid
HRP	horseradish peroxidase
hTf	human transferrin
ICP-OES	inductively-coupled plasma optical emission spectrometry
IPTG	isopropyl-β-D-1-thiogalactopyranoside
IgG	immunoglobulin isotype G
kb	kilobase pairs
kDa	kilodalton
KU	Klett unit
L	liter
LB	Luria-Bertani
M	molar
mg	milligram
mL	milliliter

Mn	manganese
mS100A7	mouse S100A7
N	Normal
N. gonorrhoeae	*Neisseria gonorrhoeae*
NaCl	sodium chloride
$NaHCO_3$	sodium bicarbonate
NaOH	sodium hydroxide
NBT	bitro-blue tetrazolium
NET	neutrophil extracellular trap
NI	nutritional immunity
OD	optical density
PBS	phosphate buffered saline
PCR	polymerase chain reaction
PID	pelvic inflammatory disease
PMN	polymorphonuclear cell
RBS	ribosome binding site
RCF	relative centrifugal force
RPM	revolutions per minute
SD	standard deviation
SDS-PAGE	sodium dodecyl-sulfate polyacrylamide gel electrophoresis
STI	sexually-transmitted infection
TBS	tris buffered saline
TdT	TonB-dependent transporter
TPEN	N,N,N’,N’-tetrakis(2-pyridinylmethyl)-1,2-ethanediamine

U	enzyme units
WCL	whole-cell lysate
WHO	World Health Organization
Zn	zinc
$ZnSO_4$	zinc sulfate
µg	microgram
µL	microliter
µM	micromolar

Abstract

CHARACTERIZATION OF THE NOVEL INTERACTION BETWEEN *NEISSERIA GONORRHOEAE* TDFJ

AND ITS HUMAN LIGAND S100A7

By Stavros Andrew Maurakis

A Thesis submitted in partial fulfillment of the requirements for the degree of Master of Science at Virginia Commonwealth University

Virginia Commonwealth University, 2018

Director: Cynthia Nau Cornelissen, Ph.D.
Professor, Department of Microbiology and Immunology

Neisseria gonorrhoeae is an obligate human pathogen that causes the common STI gonorrhea, which presents a growing threat to global health. The WHO estimated 78 million new cases of gonorrhea worldwide in 2017, with estimates of 820,000 new cases in the United States alone according to the CDC. High-frequency phase and antigenic variation inherent in *N. gonorrhoeae,* coupled with its natural ability to rapidly acquire and stably integrate antimicrobial resistance factors into its genome, have culminated in an infection against which there is no effective vaccine, and for which the list of viable therapeutic options is quickly

shrinking. Moreover, no protective immunity against subsequent infections is elicited upon exposure to *N. gonorrhoeae*, which highlights the need for research of novel antimicrobial and vaccination strategies. Within the human host, *N. gonorrhoeae* utilizes a unique strategy to overcome host sequestration of essential nutrients – termed nutritional immunity (NI) – such as ions of trace metals. The pathogen produces a family of outer membrane proteins called TonB-dependent transporters (TdTs) capable of binding to host NI factors and stripping them of their nutritional cargo for use by the pathogen. Importantly, these TdTs are very highly conserved and expressed among *Neisseria* species. TbpA is a well-characterized TdT that allows *N. gonorrhoeae* to acquire iron from human transferrin, and recent studies from our lab have shown that TdfH is capable of binding to a zinc-sequestering S100 protein called calprotectin and stripping it of its zinc ion. The S100 proteins are EF-hand calcium-binding proteins that naturally play an integral role in Ca^{2+} homeostasis, but due to their ability to bind transition metals, they have also demonstrated an innate immunity role by participating in nutrient sequestration.

The S100 proteins are expressed in all human cells, and all are capable of binding transition metals including zinc, manganese, and cobalt. Calprotectin, S100A7, and S100A12 have demonstrated an ability to hinder the infection potential of pathogenic *E. coli*, *S. aureus*, *C. albicans,* and various other pathogens via zinc sequestration. Herein, we demonstrate that *N. gonorrhoeae* is able to overcome this phenomenon and actually utilize these proteins as a zinc source *in vitro*. Furthermore, we identify S100A7 as the specific ligand for TdfJ, which utilizes this ligand to internalize zinc during infection. S100A7 growth support *in vitro* is dependent upon a functional TonB, TdfJ, and the cognate ABC transport system ZnuABC, and isogenic

mutants incapable of producing *znuA* or *tdfJ* recover S100A7 utilization by complementation. Whole-cell binding assays and affinity pulldowns show that S100A7 binds specifically to both gonococcal and recombinant TdfJ, and growth and binding experiments show that these described phenomena are specific to human and not mouse S100A7. Finally, we show that a His-Asn double mutant S100A7 that is incapable of binding zinc cannot be utilized for growth by gonococci. These data illustrate the unique nature of the gonococcus' ability to co-opt host defense strategies for its own purposes, and further identify the TdTs as promising targets for strategies to combat and prevent gonococcal infection.

Introduction

I. Genus *Neisseria*

The *Neisseria* belong to the family *Neisseriaceae*, a subset of the phylum Proteobacteria that also contains such genera as *Kingella* and *Acinetobacter*, among others (1). *Neisseria* are Gram-negative diplococci that are known to colonize mucosal surfaces of many animals, including humans (2). The *Neisseria* are nonmotile apart from twitching motility, do not produce endospores, are oxidase positive, and achieve optimum growth at 37°C and 5% CO_2. While most members of genus *Neisseria* are commensal bacteria commonly found in the human flora, two known pathogenic species, *N. meningitidis* and *N. gonorrhoeae,* commonly infect humans. In some cases, *N. lactamica* can act as an opportunistic pathogen (3). *N. gonorrhoeae* causes the eponymous STI gonorrhea and is not part of the normal flora. Rather, the disease manifests after infection of the mucosa during vaginal, oral, or anal sex (4). As a commensal bacterium, *N. meningitidis* is carried as part of the human naso- and oropharyngeal mucosa and can cause severe disease upon dissemination.

II. *Neisseria gonorrhoeae*

A. Infection

Neisseria gonorrhoeae primarily infects nonciliated epithelial cells of the urogenital mucosa. However, infection of the oro- and nasopharynx has also been observed (10). The mechanisms used to accomplish infection show gender specificity (6). The initial binding to mucosal epithelia is mediated primarily by the gonococcal type IV pilus, allowing attachment to polarized epithelial cells. This interaction is then mediated by invasion proteins such as the opacity proteins and porins, which allow the gonococcus to be engulfed by cytoskeletal rearrangements and membrane ruffling (7-8). After internalization, gonococci are able to persist intracellularly and eventually transcytose the cell, exiting via the basolateral membrane (9). Subsequent infection of subepithelial and endothelial cells facilitates *N. gonorrhoeae* entering the bloodstream and disseminating to other areas of the body. Thus, both localized and systemic infections are possible. For dissemination to be possible, the gonococcus must evade killing by host serum factors including complement, which is partially accomplished by the bacteria binding to human factor H, an inhibitor of the alternative complement pathway (11). This binding of factor H contributes to the gonococcus' ability to disseminate and be stable in serum.

B. Disease and Epidemiology

N. gonorrhoeae is the etiological agent of the STI gonorrhea. Infection can occur in both men and women, with infections in men presenting as purulent discharge and dysuria, and ascension leading to such complications as epididymitis, prostatitis, and urethritis. In women, serious manifestations such as cervicitis, pelvic inflammatory disease (PID), infertility, and

ectopic pregnancy can occur (4), and frighteningly, approximately 80% of infected women are asymptomatic (12). If left untreated, gonococcal infection can be serious or even life-threatening, as disseminated infection may occur (5). Disseminated infection occurs in roughly 1% of infected persons and presents as skin lesions at the extremities and synovial arthritis in wrists and ankles (13). Infected women may pass gonorrhea to their newborns if they are exposed to the pathogen in the birth canal. In newborns, *N. gonorrhoeae* can cause opthalmia neonatorum, a serious eye infection that, if left untreated, can lead to blindness (14). A key hallmark of gonococcal infection is that it confers no protective immunity against subsequent exposure to the pathogen (4).

Gonorrhea is a growing threat to global health. In 2017 the WHO estimated over 100 million new cases of gonorrhea worldwide (15), with 820,000 new cases occurring in the United States each year according to the CDC (16), making it the second most commonly reported STI behind chlamydia (17). Due to underreporting of the disease in less developed countries, global estimates may be low, perhaps underestimated by as much as 50% (18). The most susceptible populations are young adults and minorities, especially those that are lower on the socioeconomic scale. In the USA, the highest incidence of gonococcal disease is reported in southern states, with infection most common in African Americans, Native Americans, and Hispanics, especially those between 15-24 years of age. Rates are similar between men and women (18). Gonorrhea has implications for other diseases as well, as up to 30% of patients diagnosed with gonorrhea are also infected with chlamydia (13), and gonococcal infection has been associated with an increased amount of HIV shedding from the genital tract, making HIV-

infected persons who are also infected with gonorrhea more likely to spread HIV than someone infected with HIV alone (19).

C. Treatment and Vaccination

The current recommended treatment for gonococcal infection is dual therapy - one single intramuscular injection of 250mg ceftriaxone and 1g azithromycin taken orally (20). Rapid acquisition of antibiotic resistance among gonococcal isolates means that the list of available treatment options is rapidly shrinking. The last few decades have seen *N. gonorrhoeae* increase frequency of resistance to quinolones, and strains of gonococci showing decreased susceptibility to third-generation cephalosporins are currently being identified (21-22). In fact, 2007 marked the end of any fluoroquinolones being prescribed as treatment for gonorrhea. Even more frighteningly, a 2018 case of gonococcal disease isolated in the United Kingdom exhibited high levels of resistance to the current recommended dual therapy (23).

There is no effective vaccination against infection by *N. gonorrhoeae.* Infection does elicit a strong inflammatory response, but no protective immunity results (28). Moreover, effective cross protection by vaccines against *N. meningititis* is not confirmed. The gonococcus is a paradigm for high frequency phase and antigenic variation, creating a bacterial surface that exists in a constant state of flux and thus making identification of vaccine targets extremely difficult (24). The best model for antigenic variation in *N. gonorrhoeae* comes from the type IV pilus. This variation is mediated by non-reciprocal recombination of silent loci into the single gonococcal expression locus of pilin, *pilE*. Estimates of pilin antigenic variation range from 10^{-2} to 10^{-4} variants per CFU, with roughly 10^{7} pilin variants possible (25). Attempts at pilin-based vaccination against gonorrhea have been unsuccessful, as a vaccine composed of a single pilus

type elicited an immune response but failed to protect against gonococcal urethritis (26). A well-described model for phase variation exists in the Opacity (Opa) proteins of *N. gonorrhoeae.* The Opa proteins are invasins that interact with human CEACAMs, and are susceptible to stochastic DNA strand slippage at pentameric repeats (29). This slippage has the potential to knock Opa transcripts out of the correct reading frame, causing cessation of protein production (27). Other genes susceptible to strand slippage see changes in promoter strength and polymerase/ribosome binding. Current promising candidates for gonococcal vaccine development are a group of outer membrane transporters called TonB-dependent transporters (TdTs). These proteins play a key role in nutrient acquisition and are well conserved across gonococcal isolates.

III. Metal Acquisition

A. Iron

Almost all microorganisms require iron for survival. In the bacterial cell, iron plays a key role as a cofactor in many enzymatic reactions, and *N. gonorrhoeae* is no exception. Thus, as an invading pathogen, the gonococcus is susceptible to growth inhibition in environments containing a prohibitively low iron concentration. The human host, by use of high-affinity iron carrier proteins, restricts the serum iron concentration to approximately 10^{-24} M (30), owing partially to the fact that free iron can be toxic to cells. In terms of immunity, this iron sequestration has the effect of starving invading pathogens of the essential nutrient, a phenomenon often referred to as nutritional immunity (31). Pathogens have evolved certain mechanisms to overcome nutritional immunity, most commonly by the production of high-affinity non-ribosomally produced chelating compounds called siderophores, which are capable

of outcompeting host proteins for iron (32). Critically, *N. gonorrhoeae* does not produce siderophores, and instead employs an arsenal of TonB-dependent transporters (TdTs) capable of binding directly to host nutritional immunity proteins and stripping them of their metal cargo (33). The TdTs all consist of a β-barrel consisting of 22 amphipathic β strands, and a globular plug domain to occlude the barrel when not transporting cargo (36). The gonococcus produces eight known TdTs (Fig. 1), of which four are known to play a role in iron acquisition (34). The best characterized of these is TbpA, which allows acquisition of iron from human transferrin with the help of TbpB. All gonococcal isolates identified to date possess genes for production of TbpAB, but mutant strains incapable of producing these proteins are incapable of growth on human transferrin as a sole iron source (37). Human transferrin is a serum glycoprotein responsible for binding and transporting iron and is ~30% saturated with iron *in vivo* (35). The current model of TbpA utilization of transferrin-iron involves binding of human transferrin by TbpA with help by TbpB, whereupon iron is extracted from transferrin and interacts with the plug domain of TbpA. At this point, the TonB protein uses the proton motive force to alter the plug in a manner that promotes iron release into the periplasm, freeing it to be transported the rest of the way into the cell by a cognate ABC transport system (discussed below) (34). The basic mechanism for iron internalization is the same for the other two-component TdTs of *N. gonorrhoeae*, LbpA and HpuB. LbpA allows the gonococcus to utilize human lactoferrin as a sole iron source, but about half of gonococcal isolates have lost the ability to produce the protein (38). *N. gonorrhoeae* does not have a dedicated transport system for free heme, but the HpuB protein allows the pathogen to utilize heme bound to hemoglobin as a source of iron (39). Unlike Tbp and Lbp, the HpuAB system does not exclusively recognize human hemoglobin, but

can in fact recognize those from other mammals as well (34). The fourth iron-centric TdT of *N. gonorrhoeae* is FetA. Unlike the three transporters already discussed, FetA has no associated lipoprotein to aid in uptake efficiency. FetA has been shown to increase binding and acquisition of enterobactin when expressed (40). The siderophore enterobactin is a produced by several other bacteria and apparently can be co-opted by the gonococcus, as can other siderophores including salmochelin (41) and dihydroxybenzoylserine (34). Two additional TdTs, TdfF and TdfG, are as yet incompletely characterized. Like FetA and the other Tdfs (discussed in the next section), these two proteins lack a surface-associated lipoprotein, and both show regulation by metal ions as they are repressed by iron (47-48). TdfF is present in all pathogenic *Neisseriae* but not commensals (49), and its absence has been shown to contribute to growth defects within epithelial cells (47). TdfG is the largest TdT identified in *Neisseria* at 136kDa, and is almost completely exclusive to *N. gonorrhoeae* (49).

B. Zinc

Like iron, zinc is an essential cofactor in many enzymatic reactions critical to the survival of bacteria, such as oxidation-reduction and nucleoside biosynthesis. As such, bacterial pathogens have evolved several mechanisms of ensuring they maintain an adequate supply of this key element (42). Unsurprisingly, *N. gonorrhoeae* produces two TdTs that help the pathogen acquire zinc: TdfH and TdfJ (43-44). TdfH and TdfJ do not feature a surface-tethered lipoprotein. TdfH and TdfJ are repressed by zinc, which is consistent with the expected phenotype of a zinc transporter. TdfJ additionally is induced by iron-replete conditions. It has recently been shown that TdfH enables *N. gonorrhoeae* to utilize human calprotectin as a sole source of zinc *in vitro*.

Figure 1. TonB-dependent transporters and their associated lipoproteins and ABC transport systems produced by *Neisseria gonorrhoeae*. The TonB-dependent transporters (TdTs) of *N. gonorrhoeaea* are essential for acquiring metals such as iron and zinc. TbpA, LbpA, HpuB, and their associated surface-tethered lipoproteins, allow the pathogen to strip iron from human transferrin, lactoferrin, and hemoglobin, respectively. FetA strips iron from xenosiderophores of other bacteria. TdfH was recently shown to remove zinc from human Calprotectin, and TdfJ binds to free zinc. No ligand for TdfF or TdfG has been identified. (64)

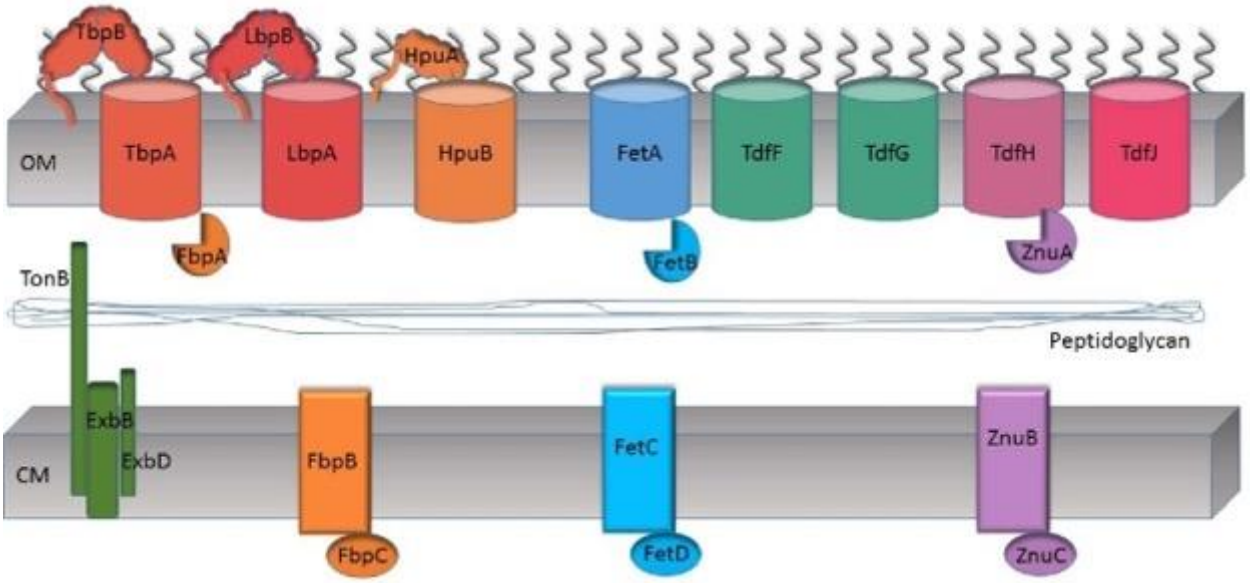
TbpB
LbpB
HpuA
OM
TbpA
LbpA
HpuB
FetA
TdfF
TdfG
TdfH
TdfJ
FbpA
FetB
ZnuA
TonB
Peptidoglycan
ExbB
ExbD
CM
FbpB
FetC
ZnuB
FbpC
FetD
ZnuC

The gonococcus binds directly to calprotectin in a TdfH-dependent manner and internalizes zinc via TonB and ABC transport (43). TdfJ is expressed by all *Neisseriae* (44). The *N. meningitidis* homologue of TdfJ, named ZnuD, has been shown to participate in both zinc and heme utilization, and is regulated by both *zur* and *fur* (45). Moreover, in a mouse model ZnuD was required to cause systemic infections by the meningococcus, and X-ray crystallography shows that free zinc ions bind directly to ZnuD (46).

C. ABC Transport of Metals

The aforementioned TdTs all rely on a cognate ABC transport system for completion of metal internalization by the bacterium. Once iron and zinc have passed through the outer membrane via one of the TdTs, they are bound by periplasmic binding proteins. These proteins then dock with permeases in the cytoplasmic membrane, which is energized by hydrolysis of ATP, allowing the ions to finally enter the cell. Tbp, Lbp, and Hpu are serviced by FbpABC, which demonstrates high-affinity iron transport (50), while ZnuABC (51) transports zinc and is functionally associated with TdfH and TdfJ (44). ZnuABC has also been shown to play a role in transport of manganese and is elsewhere in the literature referred to as MntABC (52). The FetBCD system allows internalization of enterobactin associated with FetA (40).

IV. S100 Proteins

An interesting contributor to nutritional immunity are the S100 proteins. The S100 family is made up of 24 members divided into three groups separated by the location of their functions: intracellular only, extracellular only, or both intra- and extracellular. These proteins are expressed only in vertebrates, and expression patterns vary depending on cell and tissue type.

While S100 proteins have been implicated as regulators of differentiation, apoptosis, inflammation, and other pathways (58), their primary function in eukaryotic cells is maintenance of calcium signaling and homeostasis (53). The S100 proteins all feature a calcium binding EF-hand motif (54), which consists of a helix-loop-helix structure typically present in pairs that are held together by antiparallel β strands. The S100 proteins preferentially form dimers, an action that sterically affects one of the helices in the motif, making it very rigid upon calcium binding (55). Additionally, the dimer interface of the S100 proteins, which can be hetero- or homodimeric in nature, allows for the high affinity binding of transition metals such as Zn, Mn, and Cu (56) (Fig. 2). Binding of zinc by S100B was first described in 1984 (57), and since then other members of the S100 family including S100A7 (psoriasin), S100A12 (calgranulin C), and the S100A8/A9 heterodimer (calprotecin) have also demonstrated high-affinity zinc binding. Structural analyses revealed that two His-rich, symmetrically disposed binding pockets within the dimeric forms of these proteins facilitate this interaction (59). Furthermore, one of the binding pockets of calprotectin has demonstrated the ability to bind manganese. This metal binding ability coupled with calprotectin's high expression levels in neutrophils contributes to killing of invading pathogens via nutrient sequestration (60-61). Indeed, this mechanism is not unique to calprotectin, as S100A7 has demonstrated similar killing effects for *E. coli*, *S. aureus*, and *P. aeruginosa* (62), and S100A12 has been implicated in host defense against parasites by the same mechanism (63). Perhaps unsurprisingly, *N. gonorrhoeae* has evolved a method of overcoming calprotectin-mediated nutritional immunity akin to those described for transferrin and others. Gonococcal TdfH binds calprotectin and strips it of its zinc, which is then internalized for use by the pathogen. This allows the

Figure 2. S100 family proteins involved in nutritional immunity. S100 proteins are obligate homo- or heterodimers dimers, consisting of subunits which oligomerize in the presence of micromolar concentrations of calcium. Shown above are the structures of a few members of the S100 family that have been implicated in nutritional immunity. (A) S100A7 bound to zinc. (B) S100A12 bound to copper. (C) Calprotectin bound to zinc and manganese.

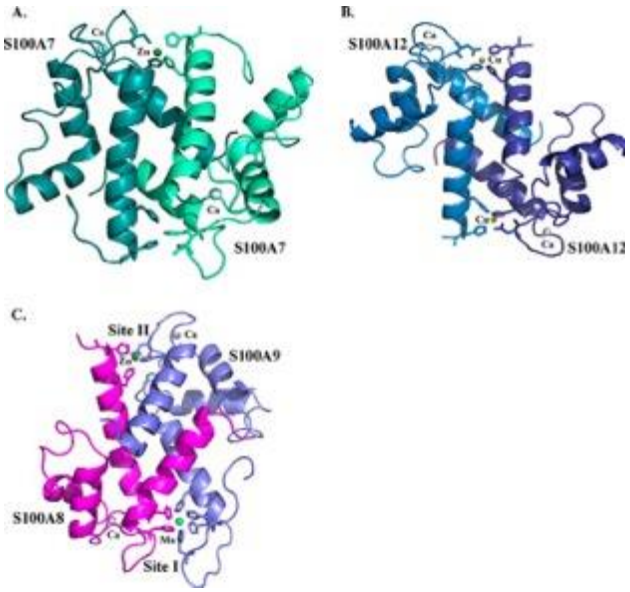
A.
S100A7
S100A7
B.
S100A12
S100A12
C.
Site II
S100A9
S100A8
Site I

gonococcus to survive in neutrophil NETs *in vitro* (43.) Based on the structural similarity of the gonococcal TdTs and that of the S100 family of proteins, coupled with the ability of S100s to bind transition metals that also regulate the TdTs, and with knowledge of an existing system for TdT-mediated zinc uptake from calprotectin, it is hypothesized that study of the other S100 proteins may contribute to identification of other human ligands for the TdTs, and ultimately further clarify the TdT's potential as promising vaccine and antimicrobial targets.

V. Research Objectives

To further characterize the gonococcal TdTs, specifically the Tdfs, and evaluate their potential as vaccine candidates, we have developed the following aims for this study:

Aim 1. Screen zinc-binding S100 proteins for the ability to support growth of *N. gonorrhoeae* as a sole zinc source, and evaluate whether any observed growth is dependent upon the Tdfs

N. gonorrhoeae has already proven itself capable of utilizing zinc bound to calprotectin as a sole zinc source *in vitro* courtesy of TdfH (43), and the similarly zinc-regulated ZnuD is known to bind directly to a zinc ion (46) and shows remarkable sequence identity with TdfJ, which suggests that this TdT is likewise associated with zinc uptake. To evaluate whether this potential uptake is associated with S100 proteins, these potential ligands will be saturated with zinc and presented to the gonococcus as a sole zinc source and growth support will be evaluated. In the event a potential interaction is identified, biophysical tests to assess binding, specificity, and zinc internalization will be performed.

Aim 2. Evaluate the contribution of ZnuABC to Tdf-associated zinc uptake.

ZnuABC binds to both zinc and manganese (51-52). The specific ligand for TdfH, calprotectin, likewise binds to zinc and manganese (56). This is consistent with the hypothesis that a functional ZnuABC is required for TdfH-mediated zinc internalization, as well as for any potential TdfJ-mediated zinc uptake. To assess the requirement for ZnuABC in this pathway, *znuA* isogenic mutants and complemented strains will be constructed and assessed for their ability to sustain Tdf-associated zinc uptake from known and experimental zinc sources.

Materials and Methods

I. Bacterial Strains and Growth Conditions

All strains of *N. gonorrhoeae* and *E. coli* utilized in this study are summarized in Table 1. Gonococcal strains were maintained on GC medium base (Difco) plates containing Kellogg's supplement 1 and 12μM $Fe(NO_3)_3$ (Sigma) (GCB plates). Strain MCV951 was maintained as described with additional supplementation of 25μM each of $ZnSO_4$ and $MnCl_2$ and 5mM D-mannitol (Sigma). MCV954 was maintained as described with addition of 500μM IPTG (Sigma). Liquid cultures of gonococci were grown in baffled sidearm flasks (Bellco) in defined medium which was pre-treated with Chelex 100 (Bio-Rad) (CDM), with appropriate supplementation for MCV951 when needed. Growth in Zn-depleted conditions was accomplished by growing cultures in CDM supplemented with 1μM N,N,N,N-Tetrakis (2-pyridylmethyl)-ethylenediamine (TPEN) (Sigma). Strains MCV954 and MCV957 were induced with 1mM IPTG during liquid growth. Cultures were grown in a 37°C incubator with shaking at 225 RPM and supplementation with 5% CO_2, and optical density was measured by a Klett™ Colorimeter. *E. coli* strains were grown in Luria-Bertani (LB) broth (Difco) supplemented with 100μg/mL carbenicillin, 34μg/mL chloramphenicol, 50μg/mL spectinomycin, or 50μg/mL kanamycin. *E. coli*

Table 1. Strains and Plasmids Used in This Study

Strain/Plasmid	Genotype/Purpose	Reference
E. coli Strains		
TOP10	F- *mcrA* Δ(*mrr-hsdRMS-mcrBC*) ϕ80*lacZ*ΔM15 Δ*lacX74 nupG recA1 araD139* Δ(*ara-leu*)7697 *galE15 galK16 rpsL*(Str^R) endA1 λ^-	Invitrogen
NovaBlue	*endA1 hsdR17* (r_{K12}^- m_{K12}^+) *supE44 thi-1 recA1 gyrA96 relA1 lac* F′[*proA*$^+$*B*$^+$ *lacI*^{q}*Z*Δ*M15*::Tn*10*] (Tet^R)	Novagen
OverExpress C41 (DE3)	F^- *ompT gal dcm hsdS*$_B$(r_B^- m_B^-)(DE3)	Lucigen
Gonococcal Strains		
FA19	Wild-type	107
MCV925	FA19 *tdfF::*Ω	79
MCV926	FA19 *tdfG::*Ω	79
MCV927	FA19 *tdfH::*Ω	79
MCV928	FA19 *tdfJ::*Ω	79
MCV650	FA19 *tonB::*Ω	108
MCV951	FA19 *znuA::*Ω from pVCU551	This study
MCV952	FA19 transformed with pVCU553	This study
MCV954	MCV952 transformed with pVCU551	This study
MCV957	MCV928 transformed with pVCU554	This study
Plasmids		
pET11a	Expression vector	Novagen
pVCU403	pUC18 + GC uptake sequence	109
pKH37	Complementation vector	82
pVCU234	pKH37 + Shine-Dalgarno Sequence	111
pVCU313	pBAD TOPO + *tdfJ*	110
pUNCH1321	pET11a + *tdfF*	110
pVCU550	pVCU403 + *znuA* fragment	This study
pVCU551	pVCU550 + Ω cassette (*znuA::*Ω*)*	This study
pVCU552	pCR2.1 TOPO + *znuA*	This study
pVCU553	pVCU234 + *znuA*	This study
pVCU554	pVCU234 + *tdfJ*	This study

liquid cultures were grown at 37°C overnight with shaking at 225 RPM, and those maintained on agar plates were incubated at 37°C overnight.

II. Molecular Techniques

PCR was performed using either high-fidelity *Taq*-based polymerases (Invitrogen) or Phusion polymerase (New England Biolabs) accompanied by primers synthesized by Integrated DNA Technologies. All primers used in this study are listed in Table 2. PCR products were purified using a Nucleospin® Gel and PCR Clean-up Kit (Macherey-Nagel) and either cloned directly into the pCR2.1-TOPO vector (Invitrogen) according to manufacturer instructions, or cloned directly into their destination vector by utilization of the In-Fusion® Cloning System (Clontech). All restriction endonucleases used were purchased from New England Biolabs, and restriction fragments were purified from agarose gels via a QIAquick Gel Extraction kit (Qiagen). Linearized vectors were treated with recombinant shrimp alkaline phosphatase (NEB) to remove unwanted 5' phosphates prior to ligation of DNA fragments by T4 DNA ligase (NEB). Ligations were incubated overnight at room temperature prior to heat inactivation of the ligase and subsequent transformation of chemically competent *E. coli*. Plasmid DNA was recovered from *E. coli* broth cultures by using a QIAprep Spin miniprep kit (Qiagen).

III. Mutant Construction

To construct an isogenic FA19 mutant strain unable to produce ZnuA, primers oVCU865 and oVCU866 were used to amplify a region of the *znuA* gene from a chromosomal prep of strain FA19. The resulting PCR product was purified and ligated into the EcoRI site of pVCU403 (109)

via the In-Fusion® cloning method. This ligation mixture was used to transform TOP10 (Invitrogen) *E. coli* and transformants were selected on 50µg/mL carbenicillin and confirmed by PCR to generate pVCU550. To disrupt the *znuA* gene, an Ω cassette (Spc^R Str^R) was ligated into the BmgB1 site of the *znuA* fragment from pVCU550 with T4 DNA ligase. This ligation was used to transform Novablue (EMD Millipore) *E. coli* and transformants were selected on 50µg/mL spectinomycin and confirmed by PCR. The resulting plasmid, pVCU551 (Fig. 3), was linearized with SspI and used to transform a piliated population of gonococcal strain FA19, creating MCV951 which was confirmed by PCR. Recovery of these transformants required GCB plates supplemented with 25µM each of Zn and Mn plus 5mM D-mannitol, in addition to selection on 50µg/mL spectinomycin. To generate an IPTG inducible *znuA* complement, primers oVCU893 and oVCU894 were used to amplify the full *znuA* gene from FA19, which was then purified and subcloned into pCR2.1 TOPO according to manufacturer instructions and used to transform TOP10 *E. coli.* The resulting plasmid, pVCU552, was digested with XmaI and HindIII to excise the *znuA* gene, which was then ligated with T4 DNA ligase into pVCU234 (111) that had previously been linearized with the same enzymes. pVCU234 inserts into an ectopic site of the gonococcal chromosome between the *aspC* and *lctP* loci. This plasmid was used to transform Novablue *E. coli* with selection on 34µg/mL chloramphenicol and the product plasmid pVCU553 was confirmed by PCR and sequencing. pVCU553 was linearized with PciI and used to transform piliated FA19, selecting on GCB plates plus 1µg/mL chloramphenicol, creating a partial diploid for *znuA.* This strain, named MCV552, was then transformed with linearized pVCU551 to retroactively disrupt the native *znuA* locus, with transformants selected on GCB plates

supplemented with 50µg/mL spectinomycin and 500µM IPTG (Fig. 4). The resultant strain, MCV954,

Table 2. Primers Used in This Study

Primer	Sequence	Purpose
oVCU865	CTCTAGAGGATCCCCCACCTCAAACTTACCCTTAT	*znuA* Disruption Fragment Forward
oVCU866	CCATGATTACGAATTGCCGAGTGCGTCGGAATA	*znuA* Disruption Fragment Reverse
oVCU893	CCCGGGCACAGGAAAACAGTTATGAA	*znuA* Complement Forward
oVCU894	AAGCTTTTATTGCTTCATCGCGTTGGTCTT	*znuA* Complement Reverse
oVCU967	TTAAAAGGAGCCCGGGATGCGACGAGAAGCCAAAATGG	*tdfJ* Complement Forward
oVCU968	CGGGCCCCCCCTCGAGAAACTTCACGTTTACGCCGCC	*tdfJ* Complement Reverse
oVCU173	GGCACCCAGCCTGCGCGAGCAGGGG	Ω Cassette Outward (Left)
oVCU174	CGCAACATCCGCATTAAAATCTAGCGAGGG	Ω Cassette Outward (Right)
oVCU900SM	CACGAACCCAGTGGACATAA	Ω Cassette Forward
oVCU901SM	GGGACAACGTAAGCACTACA	Ω Cassette Reverse
oVCU816	CTAGGCACCCCAGGCTTTACAC	pKH37 Sequencing
oVCU896	CAGACCGTTCAGCTGGATATT	CAT Marker Forward
oVCU897	CCTTGTCGCCTTGCGTATAA	CAT Marker Reverse

Figure 3. Schematic of construction of *znuA* null mutant MCV951. Primers oVCU865 and oVCU866 were used to amplify a region of the *znuA* gene which was ligated into the EcoRI site of pVCU403 via the In-Fusion® cloning method to generate pVCU550. To disrupt the *znuA* gene, an Ω cassette (Spc^R Str^R) was ligated into the BmgB1 site of the *znuA* fragment from pVCU550 with T4 DNA ligase. The resulting plasmid, pVCU551, was linearized with SspI and used to transform a piliated population of gonococcal strain FA19, creating MCV951, which was selected on 50µg/mL spectinomycin and 25µM each of zinc and manganese.

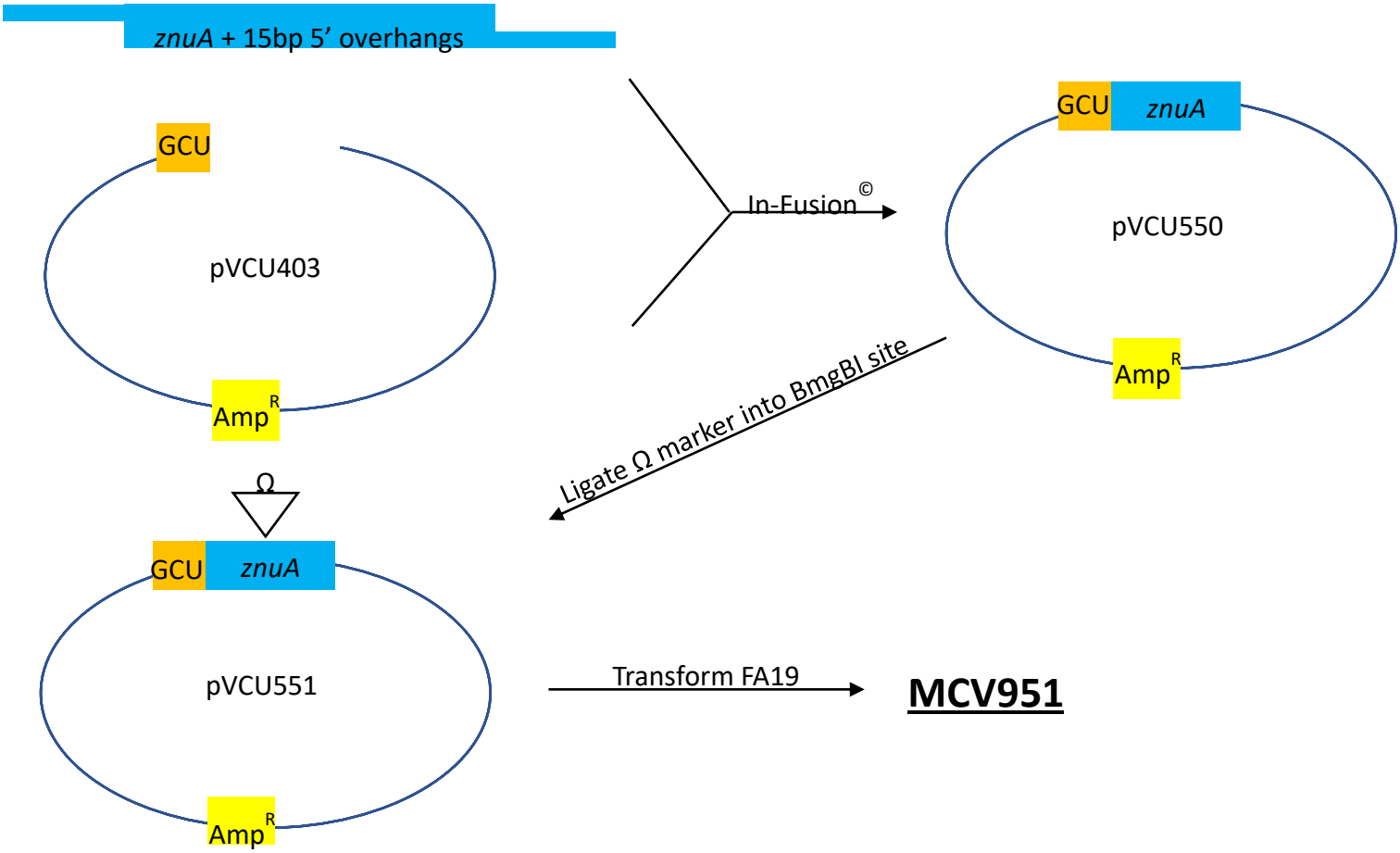
znuA + 15bp 5' overhangs
GCU
pVCU403
Amp R
In-Fusion ©
GCU znuA
pVCU550
Amp R
Ligate Ω marker into BmgBI site
Ω
GCU znuA
pVCU551
Amp R
Transform FA19
MCV951

Figure 4. Schematic representation of the construction of a *znuA* complemented strain MCV954. Primers oVCU893 and oVCU894 were used to amplify the full *znuA* gene from FA19, which was then subcloned into pCR2.1 TOPO. The resulting plasmid, pVCU552, was digested with XmaI and HindIII to excise the *znuA* gene, which was then ligated with T4 DNA ligase into pVCU234 to make pVCU553. pVCU553 was linearized with PciI and used to transform piliated FA19, selecting on GCB plates plus 1µg/mL chloramphenicol, creating a partial diploid for *znuA.* This strain, named MCV552, was then transformed with linearized pVCU551 to retroactively disrupt the native *znuA* locus, with transformants selected on GCB plates supplemented with 50µg/mL spectinomycin and 500µM IPTG. The resultant strain, MCV954, was confirmed by PCR and Southern blotting.

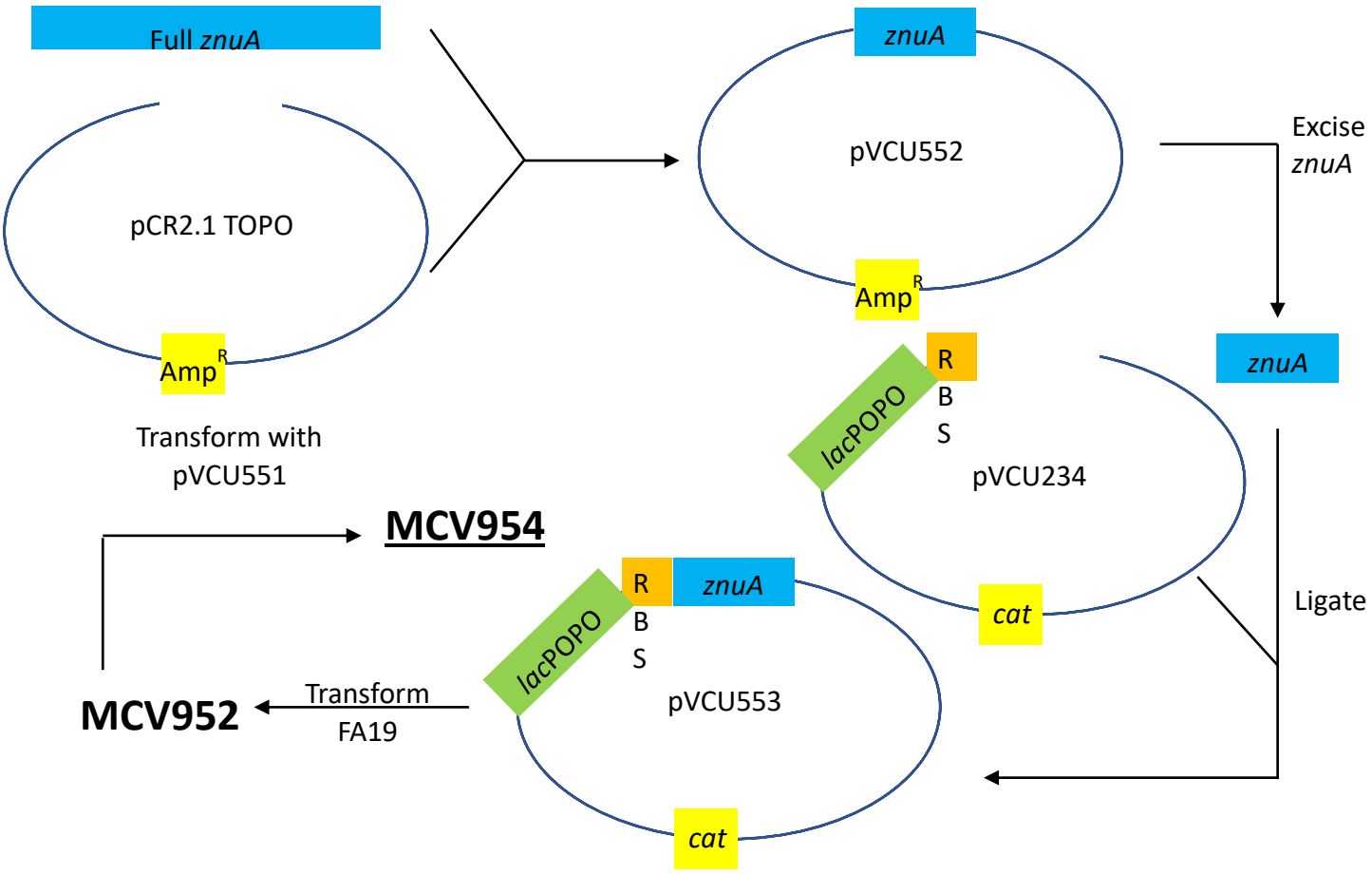
Full *znuA*
pCR2.1 TOPO
Amp R
Transform with pVCU551
znuA
pVCU552
Amp R
Excise *znuA*
znuA
R
B
S
lacPOPO
pVCU234
cat
Ligate
MCV954
R
znuA
B
S
lacPOPO
pVCU553
cat
MCV952
Transform FA19

Figure 5. Schematic of construction of *tdfJ* complemented strain MCV957. Primers oVCU967 and oVCU968 were used to amplify the full *tdfJ* gene, and generated a PCR product with 5' 15bp overhangs which were complementary to flanking regions of the complementation vector pVCU234, which inserts into an ectopic site in the gonococcal chromosome between the *aspC* and *lctP* loci. The PCR product was ligated into the XmaI and XhoI sites of pVCU234 via In-Fusion® cloning to make pVCU554, which was then linearized with PciI and used to transform MCV928. The resulting gonococcal strain, MCV957, was selected on 1µg/mL chloramphenicol and is inducible with 1mM IPTG.

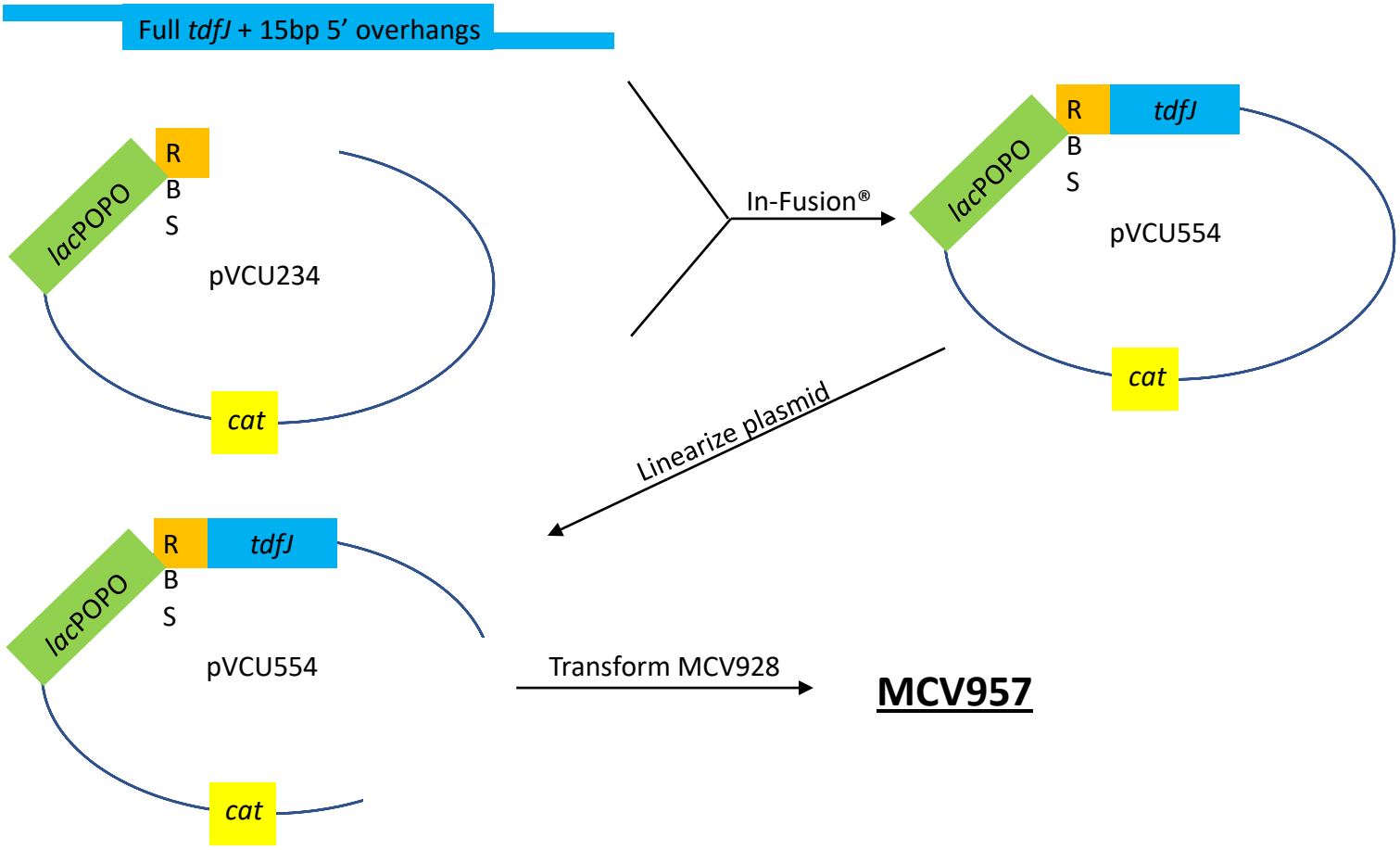
Full *tdfJ* + 15bp 5' overhangs
lacPOPO
RBS
pVCU234
cat
In-Fusion®
lacPOPO
RBS
tdfJ
pVCU554
cat
Linearize plasmid
lacPOPO
RBS
tdfJ
pVCU554
cat
Transform MCV928
MCV957

was confirmed by PCR and Southern blotting. Finally, to create an IPTG-inducible *tdfJ* complement, primers oVCU967 and oVCU968 were used to amplify the full *tdfJ* gene from FA19, which was cloned via In-Fusion® into pVCU234 that had been linearized with XmaI and XhoI and used to transform TOP10 *E. coli.* Transformants were selected on 34µg/mL chloramphenicol and confirmed by PCR and sequencing. This plasmid pVCU554 was linearized with PciI and used to transform piliated MCV928 (79), and transformants were selected on 1µg/mL chloramphenicol. The resulting strain MCV957 was confirmed by PCR and by recovery of S100A7 utilization upon IPTG induction (Fig. 5).

IV. Southern Blotting

Southern analysis of the *znuA* loci of FA19, MCV951, MCV952, and MCV954 was performed to confirm the genetic identity of MCV954. Chromosomal preps of these four strains were digested with ClaI and fully separated on a TBE-agarose gel. The gel was then transferred to an HDPE dish and covered with 0.25N HCl for 10 minutes. The gel was then denatured in 1.5M NaCl, .5N NaOH for 1h with gentle agitation. The gel was then rinsed briefly with dH_2O and washed with a solution of 0.5M Tris pH 7.0, 1.5M NaCl with gentle agitation 1h. Meanwhile, two sheets of nylon membrane and four sheets of 3MM paper were pre-soaked in 5X SSPE. After gel washing was complete, bi-directional transfer of DNA was performed at room temperature overnight. The next day, membranes were removed and UV-crosslinked with a Stratagene UV Stratalinker 2400 and added to pre-hybridization buffer (5X SSC, 1% (w/v) salmon sperm DNA, 0.1% N-lauroylsarcosine, .02% SDS) in a sealed plastic bag and incubated in a 68°C water bath for 1h. After 1h, pre-hybridization solution was replaced with hybridization

solution (as described above plus freshly-boiled PCR probe) and incubated again at 68°C with agitation overnight. The next day, filters were washed with excess 2X SSC + .1% SDS, then washed again at 68°C with excess .1X SSC +.01% SDS. Detection was performed with a Biotin Chromogenic Detection Kit (Thermo) according to the manufacturer. PCR probes were generated for *znuA* and the Ω cassette by PCR amplifying the aforementioned pieces, and were then biotinylated with a Biotin DecaLabel DNA Labeling Kit (Thermo) according to instructions.

V.Metal Loading of Proteins

Human transferrin (hTf) was dissolved in initial buffer (100mM Tris, 150mM NaCl, 20mM $NaHCO_3$, pH 8.4) prior to incubation with $FeCl_2$ at molar ratios that allow ~30% hTf saturation by Fe. This solution was then added to Slide-A-Lyzer™ dialysis cassettes (Thermo) and dialyzed against excess dialysis buffer (40mM Tris, 150mM NaCl, 20mM $NaHCO_3$, pH 7.4) for 4 hours at room temperature followed by overnight dialysis at 4°C in fresh buffer. The Fe-bound hTf was then removed via syringe and filter sterilized. S100 proteins were maintained in their own unique buffers that were present upon arrival from Dr. Chazin's lab and were loaded to ~50% saturation with Zn by incubation with $ZnSO_4$ diluted in phosphate buffered saline (PBS). This solution was combined in PBS with 30% Fe-hTf, bovine apo-transferrin (bTf), and TPEN to create a gonococcal growth "premix" which was used to restrict available zinc sources to only the S100 protein present in the growth premix. Positive control premix was made by omitting TPEN and replacing the zinc-loaded S100 protein with $ZnSO_4$ alone. Negative control premix was made by omitting any zinc source from the mix. Premixes were made as a 10X stock, and when diluted by gonococcal liquid culture, final concentrations of ingredients are as follows: 7.5µM 30% Fe-

hTf, 3µM bTf, 5µM zinc source (S100 or $ZnSO_4$), 1µM TPEN. A slight variant of this recipe was constructed to be compatible with strain MCV650, as it is unable to utilize iron bound to transferrin. In this case, bTf was omitted from the recipe, and hTf was replaced with 30µM $Fe(NO_3)_3$ (3µM final in solution).

VI. Growth of Gonococci with Zinc-bound S100 Proteins

Gonococci were grown in Zn-restricted CDM as described until exponential phase, at which point 100µL samples were added to the wells of a 96-well microtiter dish and OD_{600} was measured using a Molecular Devices Vmax kinetic microplate reader. Aliquots of liquid cultures were then diluted in CDM to OD_{600} =.02 and were used to inoculate wells of the microtiter dish that were pre-loaded with concentrated premix prepared as described above, and bringing the total volume in the wells to 100µL. In some experiments, αTdfJ IgG/sera or pre-immune IgG/sera was added to premix in amounts equimolar to the S100 protein present. At this point, another OD_{600} reading was taken and the plate was then incubated for 6h at 37°C with shaking at 225 RPM. OD measurements were taken every 2h, and graphs of data points and associated statistical analyses were performed in Graphpad Prism 7.

VII. Assay of Zinc Internalization

Gonococcal cultures were grown as described in Zn-restricted rich medium as described until doubling. After doubling, cultures were diluted and treated with 2µM S100A7 that had been pre-incubated with 1µM $ZnSO_4$, and 1mM IPTG was added if appropriate. After 6h, cultures were harvested by centrifugation at 3750 RCF for 10 minutes. The pellet was washed

with 5mL cold, Chelex-treated PBS treated with 1mM EDTA. Culture was then centrifuged and washed again for a total of two washes. This sample was added to a 15mL metal-free conical tube with 1mL set aside for protein quantification. Remaining sample was centrifuged again as described and the pellet was stored overnight at -20°C. After overnight freezing, samples were resuspended in a minimal volume of trace-metal grade (67-70%) nitric acid and transferred to 1.5mL microfuge tubes, following which they were heated to 95°C for 2h for acid digestion. After digestion, samples were transferred back to 15mL metal free conical tubes and diluted to 5% HNO_3 using Chelex-treated dH_2O. These samples were submitted for inductively coupled plasma optical emission spectrometry (ICP-OES) and trace metal profile was determined against a standard curve ranging from 5 to 4000ppb.

VIII. Whole-cell Binding Assays

S100A7 was dialyzed against excess dialysis buffer that had been modified by replacing Tris with 40mM HEPES. The protein was then conjugated to HRP using the HRP conjugation kit ab102890 (Abcam) according to the manufacturer's instructions. Gonococcal strains FA19, MCV928, and MVC957 or *E. coli* strains carrying pET11a or pVCU313 were grown as described in Zn-restricted CDM + IPTG where appropriate and LB + antibiotic, respectively. For *E. coli*, 1mM IPTG and .02% arabinose were added to pET11a and pVCU313, respectively, when OD=.5 was reached. Cultures were grown for 4h following induction before standardized culture densities were applied to nitrocellulose in a dot blot apparatus for solid-phase binding. Unbound cells were washed away with low salt TBS + 0.05% polysorbate 20, and then blocked for 1h in 5% (w/v) nonfat milk in TBS. Following blocking, S100A7-HRP was diluted to 0.2µM in blocker,

added to samples, and incubated with shaking for 1h. After incubation, samples were washed five times with low salt TBS + .05% polysorbate 20 and colorimetric detection was performed. For solid phase experiments, detection was performed using a Metal Enhanced DAB Substrate Kit (Thermo), or for ELISA by using TMB substrate solution that was stopped by addition of .16M H_2SO_4 and output read by measuring OD_{420} on a Vmax microplate reader. For competition assays, nitrocellulose was treated with bacteria as described above, and S100A7-HRP was added simultaneously with either 10-fold molar excess mouse S100A7 (mS100A7) or unlabeled human S100A7, and blots incubated were developed as described.

IX. Affinity Pulldowns

S100A7 was dialyzed against HEPES-based dialysis buffer and then coupled to Affi-Gel® 15 (Bio-Rad) according to manufacturer instructions. After coupling, remaining unreacted groups were blocked by addition of 1M ethanolamine for 1h, followed by washing with the dialysis buffer. To generate a control affinity matrix with no conjugate, the Affi-Gel® was incubated with 1M ethanolamine only and resuspended in dialysis buffer after washing. *E. coli* cultures carrying pET11a, pVCU313, and pUNCH1321 were grown in LB and induced at OD=~.5. Induction was allowed to proceed for 4h, after which cells were pelleted by centrifugation at 15000 RPM in a Sorvall RC-5B Refrigerated Superspeed Centrifuge. These pellets were then solubilized in lysis buffer (.1M Tris, .05M NaCl, 1% Triton X-100, 25µM lysozyme, 25U benzoase nuclease, pH 8.0). Solubilized *E. coli* was then passed over prepared affinity matrices at standardized amounts, and matrices were washed with dialysis buffer + 0.05% lauryl-maltoside. For specific elution of proteins bound to affinity matrix, the matrix was resuspended in 2X

Laemmli buffer containing 5% β-mercaptoethanol and boiled for 5 minutes. This product was centrifuged for 1 minute at 10,000 RPM, and the supernatants were submitted to SDS-PAGE and Western analysis.

X. SDS-PAGE and Western Analysis

Strains of *N. gonorrhoeae* or *E. coli* were grown as described before. Cultures of standardized cell density were collected and pelleted by centrifugation at 13,000 RPM. These pellets were resuspended in 100µL 2X Laemmli buffer containing 5% β-mercaptoethanol and boiled for 5 minutes. 20µL of sample was then loaded onto 7.5 or 15% polyacrylamide gels alongside 5µL Precision Plus Protein™ Markers (Bio-Rad) and run in Tris-Glycine SDS buffer until the dye fronts traversed the gel. Protein samples were then transferred to nitrocellulose and blots were Ponceau stained to demonstrate equal loading. Blots were then blocked 1h in 5% nonfat milk (w/v) in TBS. After blocking, primary antibodies (αTdfJ, αTdfF, or αS100A7) were diluted in blocker and added to membrane for 2h. Blots were washed 3X10min before addition of secondary antibodies (Goat αGuinea Pig, αRabbit, or αMouse, respectively) for 1h. Secondaries were either conjugated to alkaline phosphatase or HRP and all were purchased from Abcam. After washing, AP conjugates were developed with NBT-BCIP (Sigma) or ECL (Thermo). All chemiluminescent and colorimetric images were recorded using a Bio-Rad ChemiDoc Imaging System.

Results

I. S100 Proteins Support Growth of Wild-type *Neisseria gonorrhoeae* When Presented as a Sole Zinc Source

Neisseria gonorrhoeae utilizes a family of outer membrane proteins called TonB-dependent transporters (TdTs) in order to acquire essential nutrients from its human host. Calprotectin is a member of the S100 family of proteins and has been demonstrated to exhibit antimicrobial effects on invading pathogens including *Escherichia coli, Staphylococcus aureus,* and *Candida albicans* by means of zinc sequestration (60, 61, 66-71). Our lab recently showed that the gonococcal TdT TdfH is capable of binding Calprotectin and stripping it of its zinc, which is internalized by the pathogen (43). Like Calprotectin, many other members of the S100 protein family are able to bind zinc (56), so we sought to determine whether additional S100 proteins were able to act as a zinc source for *N. gonorrhoeae in vitro.* To assess this, we loaded S100 proteins, which had been purified as previously described (60), with zinc at a 2:1 molar ratio to accomplish ~25% zinc saturation by weight. These proteins were provided to gonococcal strain FA19 as a sole zinc source in zinc-restricted conditions, and growth was tracked over 6h. All S100 proteins utilized in this assay, which include S100A2 (72), S100A4 (73), S100A6 (74), S100A7 (75), S100A12 (76), and S100B (77), were able to support growth of the

Figure 6. Growth support of *N. gonorrhoeae* by various S100 proteins. Strain FA19 was grown in zinc-restricted CDM as described, and was treated with growth premix containing the indicated S100 protein that has been pre-treated with zinc. Growth was allowed to proceed for 6h, with OD_{600} measurements taken every 2h. A two-way repeated measure ANOVA with Tukey's correction was performed on these data, but due to clutter the results are not shown graphically. All S100 proteins except S100A4 reached significance compared to samples treated with no zinc.

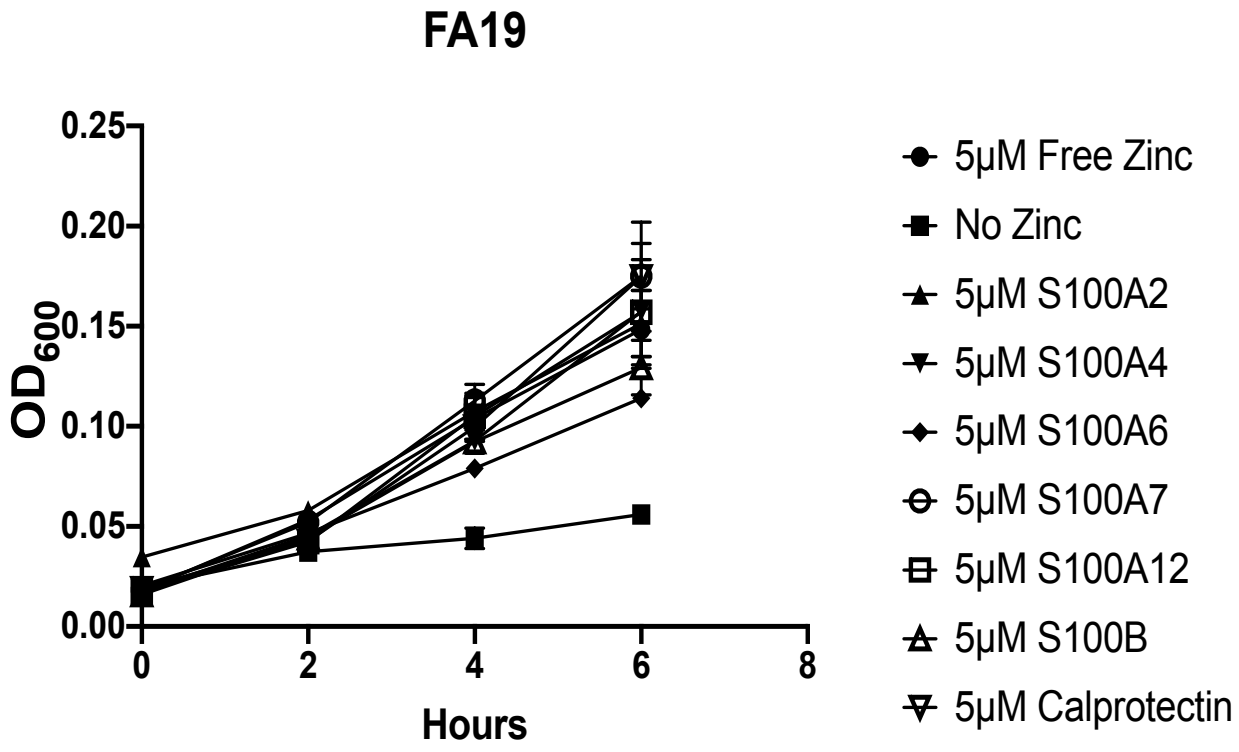
FA19
0.25
0.20
0.15
0.10
0.05
0.00
OD600
0
2
4
6
8
Hours
5μM Free Zinc
No Zinc
5μM S100A2
5μM S100A4
5μM S100A6
5μM S100A7
5μM S100A12
5μM S100B
5μM Calprotectin

gonococcus when compared to FA19 treated with no zinc, and all except S100A4 reached significance (Fig. 6). Calprotectin is known to support growth in this manner (43), so it as well as free $ZnSO_4$ were included as positive controls.

II. Strain MCV928 Cannot Utilize S100A7 as a Sole Zinc Source

We next wanted to assess whether any of the other Tdfs (F, G, and J) were involved in utilization of the S100 proteins, as is the case for TdfH and Calprotectin. To address this, we employed strains MCV925, MCV926, and MCV928, which are null mutants for *tdfF, tdfG,* and *tdfJ,* respectively. These strains were grown as described for strain FA19 and were provided with the aforementioned S100 proteins as the zinc source. Strains MCV925 and MCV926 showed an identical phenotype to strain FA19 (data not shown), while MCV928 was unable to grow when S100A7 was the sole zinc source (Fig. 7). This suggests that TdfJ is required for S100A7 to be utilized. To confirm this finding, growth with MCV928 was repeated to test only S100A7, and the previous result was recapitulated (Fig. 8). In all cases, growth of this strain was statistically indistinguishable from samples treated with no zinc.

III. Strain MCV650 Retains Growth Support by S100A12, but is Unable to Utilize S100A7

To further explore the role of TdfJ in utilization of S100A7, we performed growth assays with gonococcal strain MCV650, which is incapable of producing TonB. Despite TdfJ presence in this strain, it will not perform any transport function without a functional TonB (78). When MCV650 was grown in zinc-restricted conditions with S100A7 as a zinc source, its optical

Figure 7. *Neisseria gonorrhoeae* requires a functional TdfJ to utilize S100A7 as a sole zinc source. Strain MCV928 was grown in zinc restricted CDM as described and treated with growth premix supplemented with the designated S100 protein and were grown for 6h, with OD_{600} measurements taken every 2h.

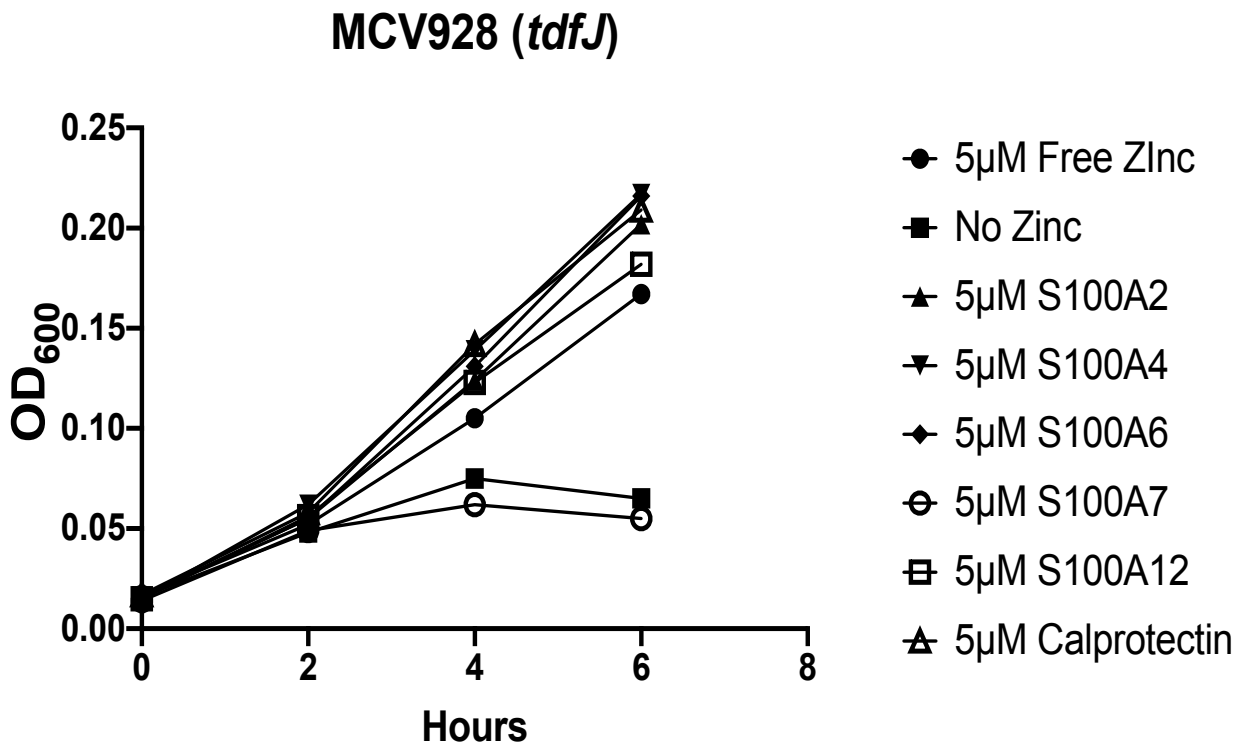
MCV928 (tdfJ)
0.25
0.20
0.15
0.10
0.05
0.00
OD600
0
2
4
6
8
Hours
5μM Free ZInc
No Zinc
5μM S100A2
5μM S100A4
5μM S100A6
5μM S100A7
5μM S100A12
5μM Calprotectin

Figure 8. MCV928 cannot utilize S100A7. (A) The *N. gonorrhoeae tdfJ* null mutant, MCV928, was grown in Zn-restricted CDM supplemented with growth premix containing $ZnSO_4$, S100A7, or no zinc. Growth was measured by OD_{600} readings every 2h for 6h total. A 2-way repeated measures ANOVA with Tukey's correction was performed for all means, with significance at 6h shown. *, P ≤. 05; **, P ≤ .005; ***, P ≤ .0005; ****, P ≤ .0001

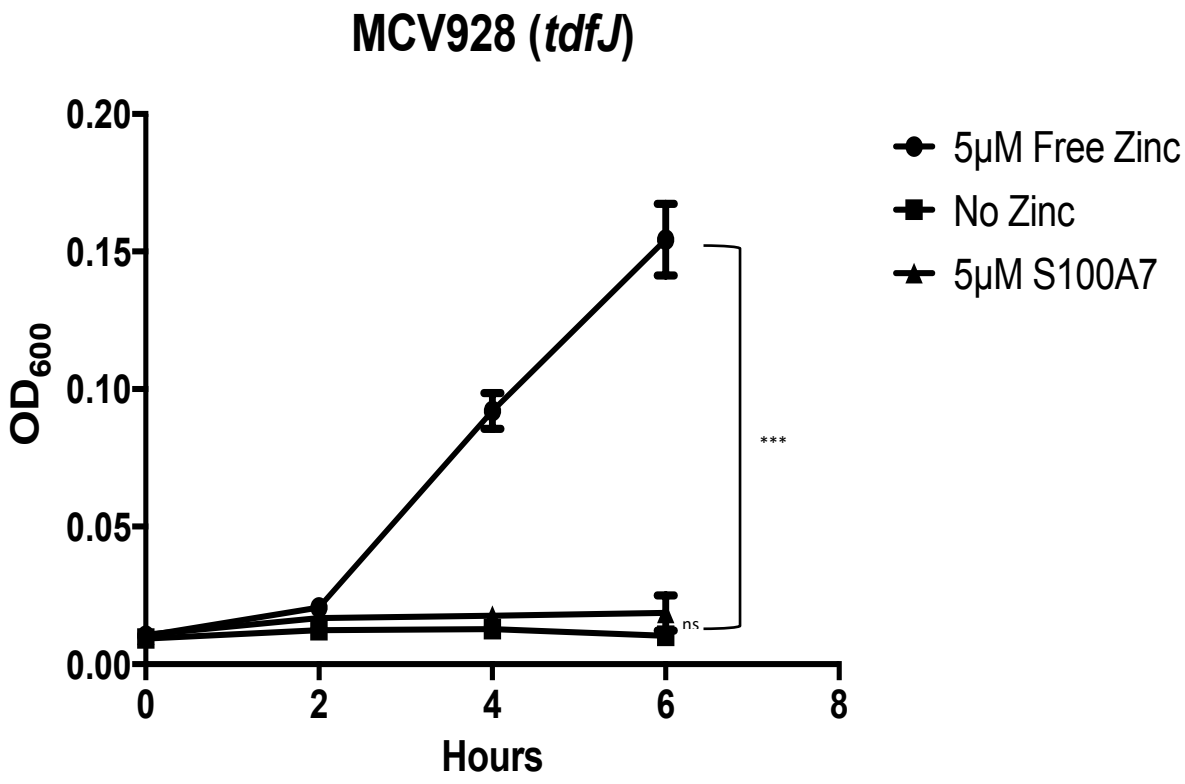
MCV928 (tdfJ)
0.20
0.15
0.10
0.05
0.00
OD600
0
2
4
6
8
Hours
***
ns
5μM Free Zinc
No Zinc
5μM S100A7

Figure 9. S100A7 utilization during growth depends on TonB. *N. gonorrhoeae* mutant strain MCV650 (*tonB*) was also grown in Zn-restricted CDM, but to overcome the mutant's inability to utilize iron from human transferrin, growth premix was instead prepared with 3µM $Fe(NO_3)_3$ with iron chelators excluded. Both graphs demonstrate means and SD for n=3 independent experiments. A 2-way repeated measures ANOVA with Tukey's correction was performed for all means, with significance at 6h shown. *, P ≤. 05; **, P ≤ .005; ***, P ≤ .0005; ****, P ≤ .0001

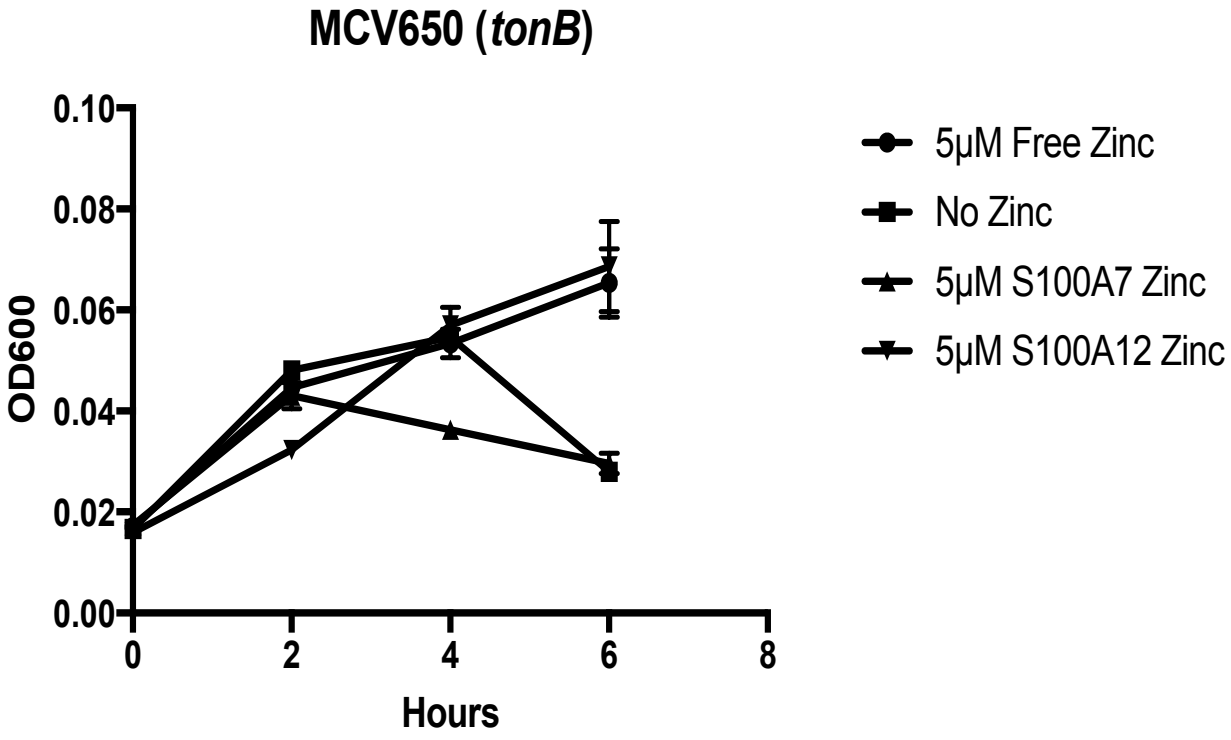
MCV650 (*tonB*)
0.10
0.08
0.06
0.04
0.02
0.00
OD600
0
2
4
6
8
Hours
5μM Free Zinc
No Zinc
5μM S100A7 Zinc
5μM S100A12 Zinc

density at 6 hours was indistinguishable from a strain treated with no zinc (Fig. 9). S100A12, which according to previous experiments does not depend on a TdT for growth support, was included in this experiment as well for comparison to S100A7. At 6h, samples treated with S100A12 reached higher optical densities than seen in samples treated with free zinc, suggesting its utilization does not depend on TonB or the TdTs. While a mechanism for this was not investigated in these studies, Ton-independent utilization of siderophores by gonococci has been described (79).

IV. TdfJ is Zinc Repressed and Iron Induced in Strain FA19

Previous reports have established that in strain another wild-type strain, FA1090, TdfJ production is repressed by zinc and induced by iron (43), but the regulatory effects of these metals were only considered individually and not in concert with each other, and not in strain FA19. We sought to identify the regulatory pattern of TdfJ in strain FA19 as concerns these metals, both alone and together. We performed Western analysis of whole-cell lysates prepared from strain FA19 grown in chemically defined media (CDM) supplemented with zinc, iron, and/or the high affinity zinc chelator TPEN at the concentrations indicated (Fig. 10). We found that levels of TdfJ were decreased in the presence of zinc and increased in the presence of iron. TdfJ production was almost nonexistent when zinc was present and iron absent, which agrees with the observed phenotype for FA1090. When grown in iron-rich and zinc-deplete conditions, TdfJ production was maximal. We confirmed equal sample loading by Ponceau S, and with these results established a set of conditions that are optimal for TdfJ production. These conditions were utilized for all experiments requiring maximal expression of the protein.

Figure 10. TdfJ is zinc repressed and iron induced. Strain FA19 was grown in CDM until exponential growth, then back diluted in the same media and treated with $Fe(NO_3)_3$, $ZnSO_4$, and/or TPEN in the concentrations indicated. These cultures were grown for 4 hours before whole-cell lysates of equalized density were prepared and subjected to SDS-PAGE and subsequent immunoblotting with antiserum raised against TdfJ. Ponceau stained blot shows equal sample loading.

Fe (µM)	**-**	**24**	**-**	**24**
Zn (µM)	**10**	**10**	**-**	**-**
TPEN (µM)	**-**	**-**	**1**	**1**

TdfJ

Ponceau S

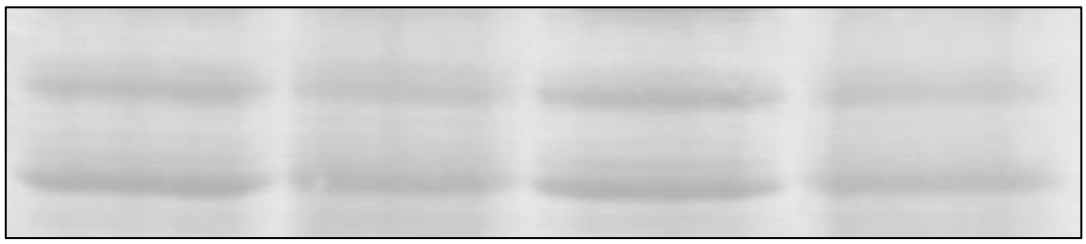

V. S100A7 Utilization is Recovered in an Induced *tdfJ* Complemented Strain *In Vitro*

Having established that absence of endogenous TdfJ in *N. gonorrhoeae* resulted in loss of growth support by S100A7, we sought to demonstrate IPTG-inducible complementation of *tdfJ* by inserting a functional version of the gene in an ectopic site in the chromosome of MCV928. We utilized the In-Fusion® cloning method to insert the full *tdfJ* sequence into pVCU234, which is a modified version of pKH37 containing a consensus Shine-Dalgarno sequence (80) as the beginning of the polylinker. pVCU234 contains two copies of the *lac* promoter region (81) and inserts between the *aspC* and *lctP* loci (82) in the gonococcal chromosome, allowing us to insert the construct directly into the *tdfJ* null strain MCV928. This process is illustrated in figure 5, and strain identity was confirmed by PCR and named MCV957.

We next utilized MCV957 in growth assays identical to those previously described to determine whether it could recover utilization of S100A7. When induced with 1mM IPTG, MCV957 completely recovers the growth phenotype for S100A7 that was observed in the wild-type, while uninduced samples were indistinguishable from samples grown with no zinc (Fig. 11). Based on these data in conjunction with data from strains MCV928 and MCV650, we concluded that a functional TdfJ is required for S100A7 utilization.

VI. S100A7 Binds Both Gonococcal and Recombinant TdfJ

Having established that TdfJ is required for S100A7-dependent growth, we next wanted to establish whether a physical protein-protein interaction was present between the two. To address this, we grew gonococcal strains FA19, MCV928, and MCV957 with and without IPTG in zinc-restricted CDM before bacteria of standardized optical density were applied to a

Figure 11. A *tdfJ* complemented strain, MCV957, recovers S100A7-dependent growth when induced. MCV957 was grown as described previously, with S100A7-containing premixes further supplemented with either 1mM IPTG or no IPTG. The graph demonstrate means and SD for n=3 independent experiments. A 2-way repeated measures ANOVA with Tukey's correction was performed for all means, with significance at 6h shown. *, P ≤. 05; **, P ≤ .005; ***, P ≤ .0005; ****, P ≤ .0001

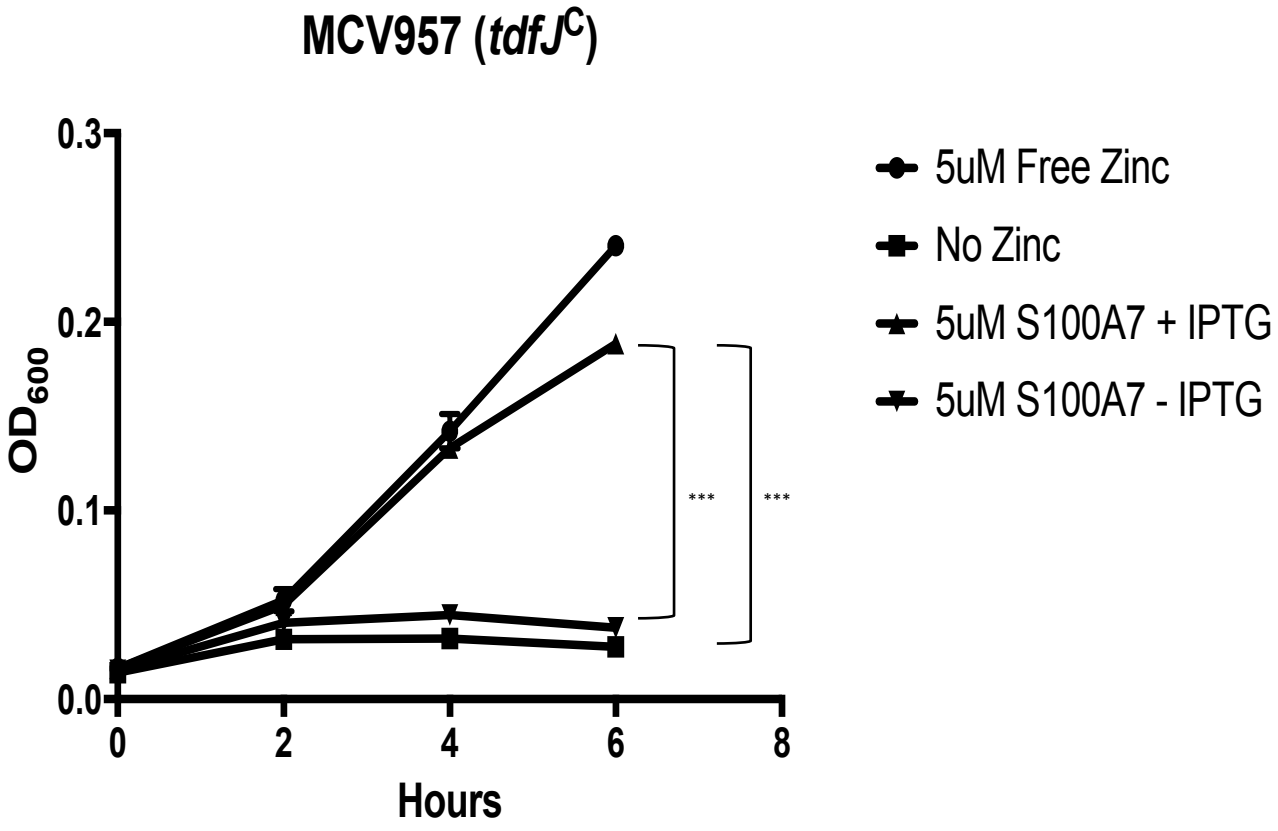
MCV957 (tdfJC)
0.3
0.2
0.1
0.0
OD600
0
2
4
6
8
Hours
***
***
5uM Free Zinc
No Zinc
5uM S100A7 + IPTG
5uM S100A7 - IPTG

nitrocellulose membrane in a dot blot apparatus. This method allowed us to probe the surface of bacterial proteins presenting surface antigens in their native conformation. When probed with HRP-labeled S100A7, only strains FA19 and induced MCV957 demonstrated detectable binding upon signal development (Fig. 12). These results demonstrate that not only is wild-type *N. gonorrhoeae* capable of directly binding S100A7, but that TdfJ is necessary for this interaction. To address the fact that possible disruption of the native gonococcal outer membrane may have occurred upon deletion of TdfJ, we wanted to recapitulate these findings in *E. coli* producing recombinant TdfJ. We induced cultures of *E. coli* harboring either pVCU313 for *tdfJ* expression or an empty expression vector pET11a and applied them to nitrocellulose at the same optical densities used for gonococci before probing with S100A7-HRP in the same manner described above. Only *E. coli* displaying TdfJ on their surface generated detectable signal.

We next sought to demonstrate these binding interactions by affinity pulldowns. We first conjugated S100A7 to Affi-Gel 15® and blocked any unreacted groups by addition of 1M ethanolamine, or made a null matrix by blocking all reactive groups without any conjugate added. We next induced *E. coli* containing pVCU313 (*tdfJ)*, pUNCH1321 (*tdfF),* or empty pET11a and passed solubilized lysates of these cultures over the matrices. Specific eluates from the matrices were isolated after washing and these fractions were analyzed by SDS-PAGE and Western blotting (Fig. 13). TdfJ was specifically eluted from only the matrix conjugated to S100A7, and TdfF did not bind this matrix. Neither protein was bound to the null matrix. We therefore concluded that S100A7 directly binds TdfJ.

Figure 12. S100A7 binds both gonococcal and recombinant TdfJ. *N. gonorrhoeae* strains FA19, MCV928, and MCV957 with and without IPTG were grown as described in Zn-restricted CDM supplemented with 24μM $Fe(NO_3)_3$ for 4 h before being applied to nitrocellulose in a dot blot apparatus at a standardized optical density (top row). *E. coli* strains containing pVCU313 for TdfJ production or carrying an empty pET11a vector were grown in LB and induced for 4h before standardizing to the same optical density as used for gonococci and subsequently applied to nitrocellulose (bottom right). Samples were blocked and then probed for 1 h with HRP-labeled S100A7 diluted in blocker before colorimetric development. Wells lacking culture were probed with S100A7-HRP and developed to determine background signal (bottom left).

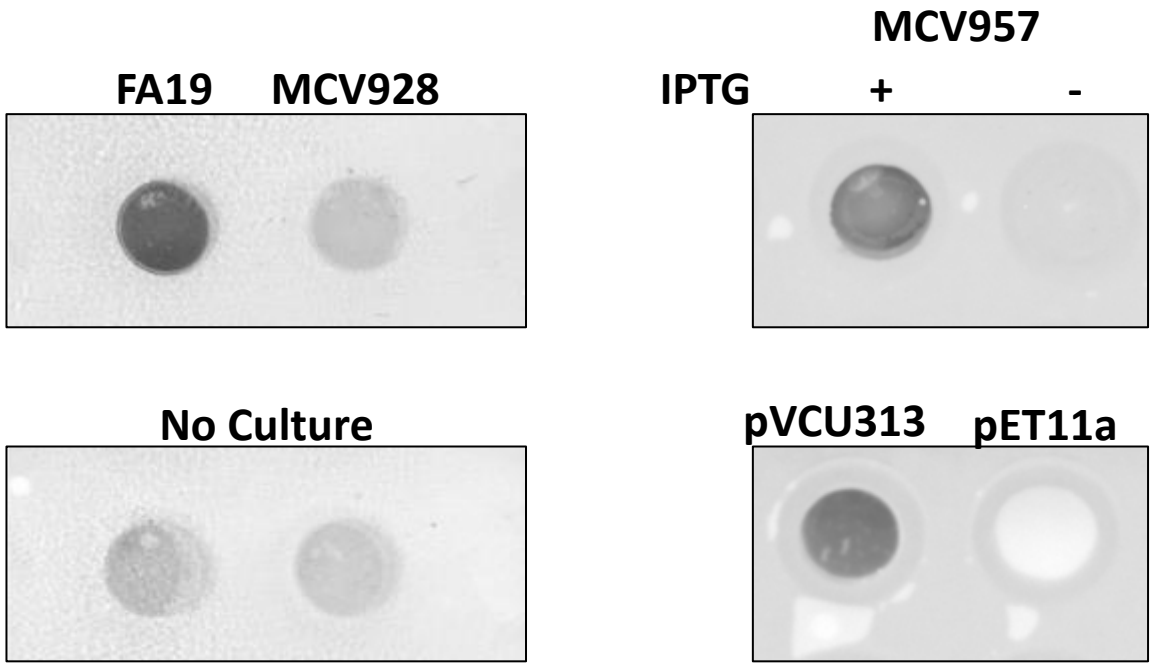
FA19
MCV928
MCV957
IPTG
+
-
No Culture
pVCU313
pET11a

Figure 13. Recombinant TdfJ is specifically eluted from an S100A7-conjugated affinity matrix. Solubilized recombinant *E. coli* strains pVCU313 or pUNCH1321 expressing TdfJ and TdfF, respectively, or an empty vector were passed over Affi-Gel 15 affinity matrix conjugated with S100A7 or a fully-blocked null matrix with no S100 protein. Nonspecific proteins from lysates were removed by washing prior to specific elution and identification by SDS-PAGE and Western Blotting.

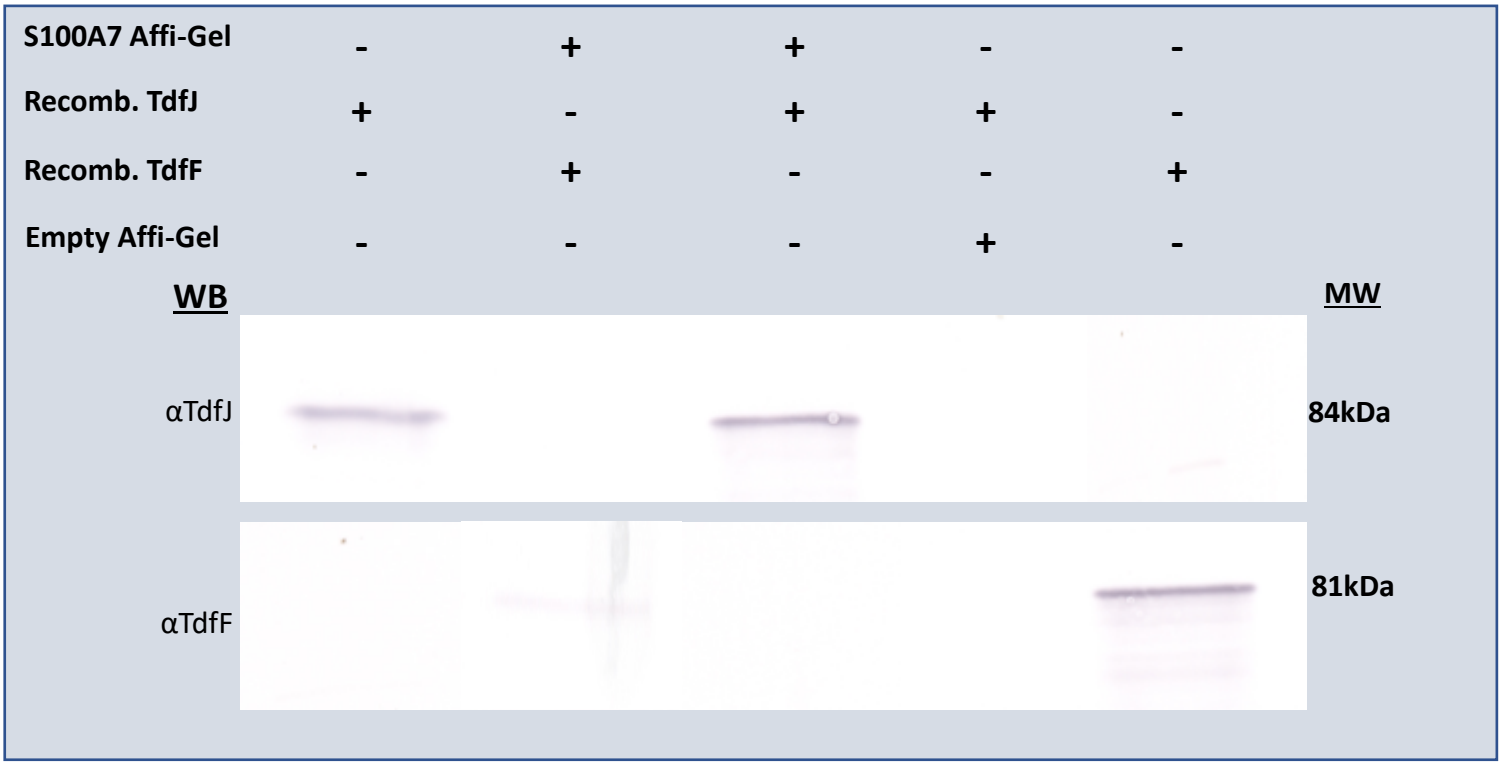
S100A7 Affi-Gel - + + - -
Recomb. TdfJ + - + + -
Recomb. TdfF - + - - +
Empty Affi-Gel - - - + -
WB
MW
αTdfJ
84kDa
αTdfF
81kDa

VII. TdfJ Interacts Specifically With the Human Version of S100A7

Neisseria gonorrhoeae is an obligate human pathogen, and as such has evolved in many ways to specifically interact with the human host (83). We sought to determine whether the same was true for the S100A7/TdfJ interaction. The mouse version of S100A7 (mS100A7, Abbexa) was loaded with zinc at the same saturation used for the experiments conducted with human S100A7 and presented to wild-type FA19 cells as a sole zinc source in otherwise zinc-depleted media. mS100A7 was completely unable to support growth of gonococci, demonstrating optical densities even lower than those samples given no zinc source (Fig 14). As mS100A7, like the human version, sequesters zinc, it is feasible that this further diminished growth phenotype is due to additional, effective zinc chelation by mS100A7 during the assay as there is no mechanism present for the gonococcus to circumvent this.

In addition to growth restriction, we tested the ability of gonococci and recombinant E. coli to physically bind mS100A7 by performing competition assays. FA19, MCV928, and MCV957 with and without IPTG, or *E. coli* expressing *tdfJ* or an empty vector were dotted onto nitrocellulose in standardized amounts before blocking and probing with S100A7-HRP. Simultaneously with the ligand, we added 10-fold molar excess of either mS100A7 or unlabeled human S100A7 as competitor. As before, only those cultures presenting TdfJ on the surface generated any signal from HRP, and only samples treated with human competitor demonstrated signal reduction;

Figure 14. TdfJ utilization of S100A7 is specific for the human version of S100A7. Strain FA19 was grown in Zn-restricted CDM supplemented with growth premix containing $ZnSO_4$, human S100A7, mouse S100A7, or no zinc. OD_{600} readings were taken every 2h for 6h total. Mean and SD for n=3 experiments are represented in the graph. A 2-way repeated measures ANOVA with Tukey's correction was performed for all means, with significance at 6h shown. *, P ≤. 05; **, P ≤ .005; ***, P ≤ .0005; ****, P ≤ .0001

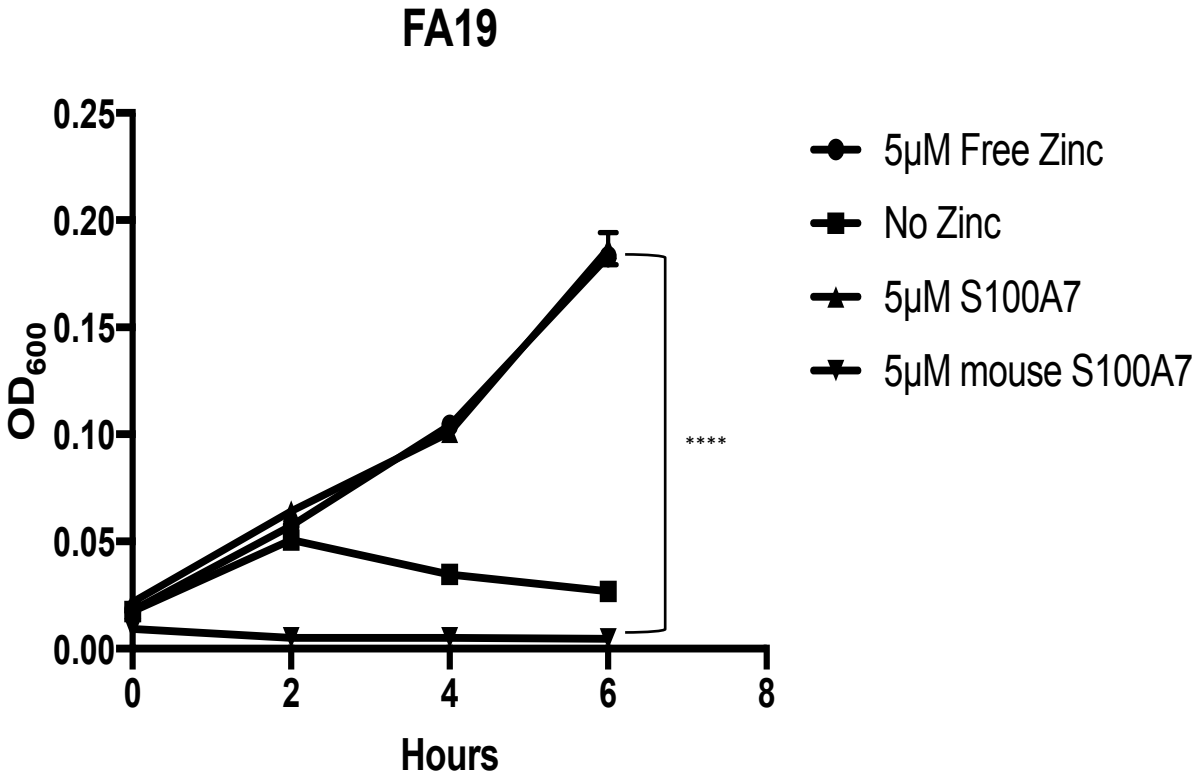
FA19
0.25
0.20
0.15
0.10
0.05
0.00
OD600
0
2
4
6
8
Hours
****
5μM Free Zinc
No Zinc
5μM S100A7
5μM mouse S100A7

Figure 15. TdfJ binds only to the human version of S100A7. Strain FA19 and MCV928 (*tdfJ*) were grown in Zn-restricted CDM supplemented with 24μM $Fe(NO_3)_3$ for 4 hours, after which equal culture densities were transferred to nitrocellulose in a dot blot apparatus. *E. coli* containing pVCU313 for TdfJ production or an empty pET11a were grown in LB and induced for 4h before being standardized to the same optical density used for gonococci and applied to nitrocellulose. Blots were then blocked and subsequently treated with HRP-labeled S100A7 either alone or with a 10-fold molar excess of unlabeled mouse or human S100A7 as competitor. Following this treatment blots were washed and colorimetric signal detection performed. Blots shown are representative of n=3 experiments.

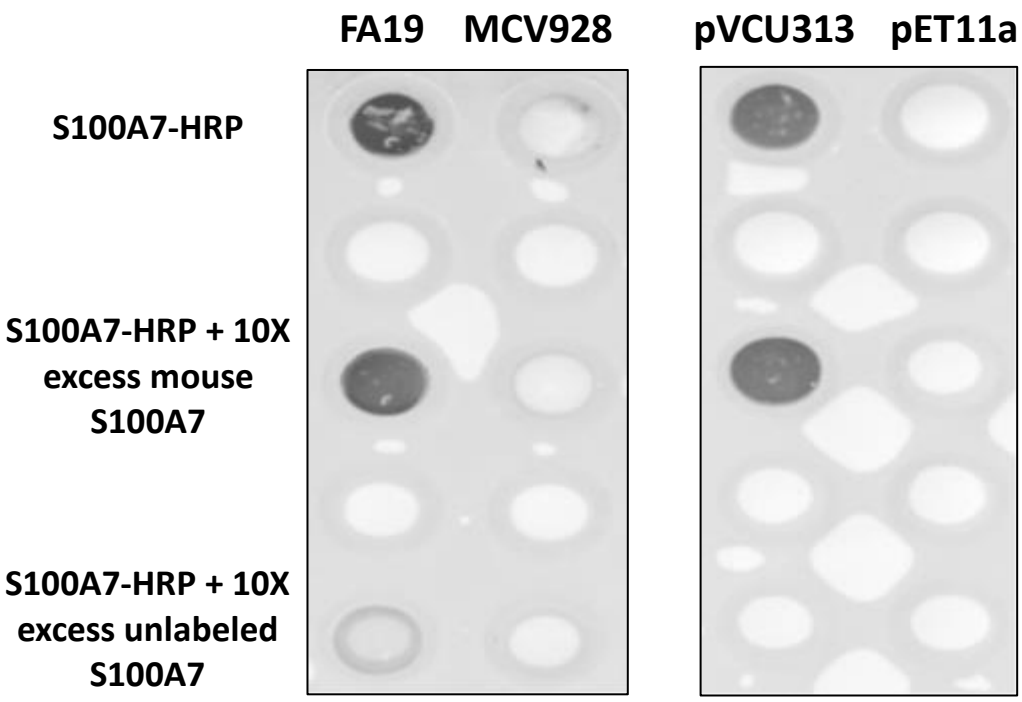
FA19
MCV928
pVCU313
pET11a
S100A7-HRP
S100A7-HRP + 10X excess mouse S100A7
S100A7-HRP + 10X excess unlabeled S100A7

mS100A7 did not compete for binding of gonococcal TdfJ (Fig 15). These data are consistent with the conclusion that the TdfJ/S100A7 interaction, like other gonococcal surface structure/host ligand interactions, is specific to the human host, consistent with *N. gonorrhoeae's* nature as an obligate human pathogen.

VIII. TdfJ Allows *Neisseria gonorrhoeae* to Internalize Zinc From S100A7

Having demonstrated that S100A7 both binds to TdfJ and supports growth as a zinc source, we next wanted to ascertain whether this pathway led to accumulation of zinc within *N. gonorrhoeae.* We grew strains FA19, MCV928, and MCV957 with and without IPTG in zinc-restricted rich medium in the presence of partially zinc-saturated S100A7 before quantifying the amount of zinc assimilation by using inductively coupled plasma optical emission spectrometry (ICP-OES). A schematic illustration of the ICP-OES process is shown in Figure 16. Zinc concentrations were determined as counts/second measured at 213.857 nm and then standardized to reflect µg zinc per mg cellular protein (Fig. 17). Strain FA19 internalized significantly more zinc from S100A7 than was seen for MCV928, suggesting TdfJ is necessary for this process. IPTG-induced MCV957 similarly showed significantly more zinc assimilation than both MCV928 and uninduced MCV957, which agrees with our previous experiments that showed complementation of *tdfJ* recovers both gonococcal binding of and growth support by S100A7. These data demonstrate that gonococcal TdfJ interacts with S100A7 in a manner that facilitates zinc internalization by the pathogen.

Figure 16. A schematic representation of the ICP-OES process.

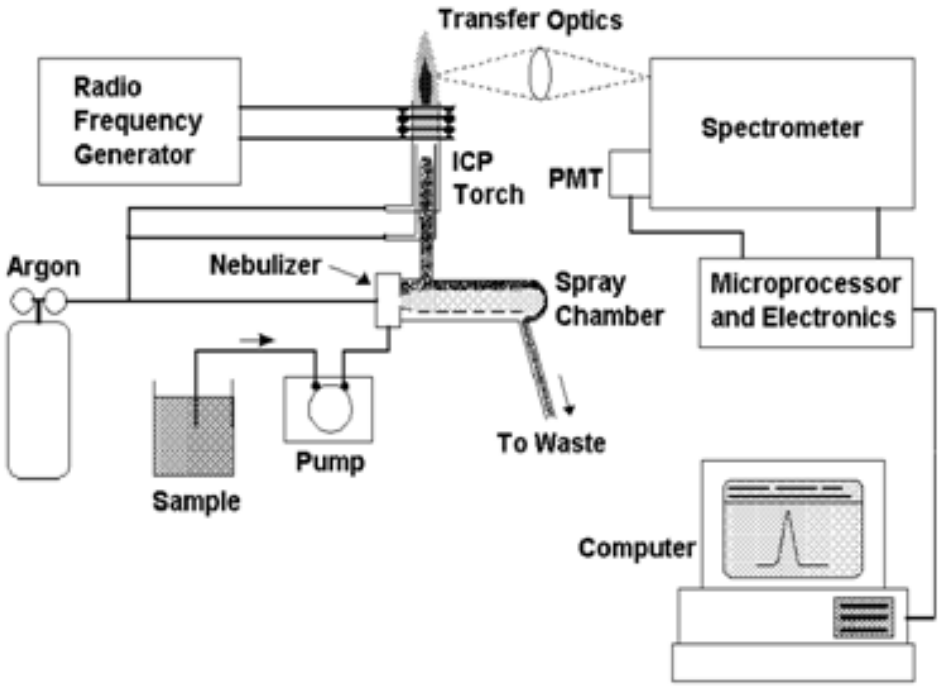
Transfer Optics
Radio
Frequency
Generator
Spectrometer
ICP
Torch
PMT
Argon
Nebulizer
Spray
Chamber
Microprocessor
and Electronics
To Waste
Pump
Sample
Computer

Figure 17. TdfJ internalizes zinc from S100A7. Strains FA19, MCV928 (*tdfJ*), and MCV957 ($tdfJ^{C}$) with and without IPTG were grown in Zn-restricted rich medium supplemented with 2uM partially-saturated S100A7. After 6h cells were harvested and digested in concentrated TMG nitric acid prior to ICP-OES analysis to detect trace metals profile. Data shown are measured counts/second read at 213.857nm per mg cellular protein compared to a trace metals standard curve ranging from 5 to 4000ppb. N=3 independent cultures. *, P ≤. 05; **, P ≤ .005; ***, P ≤ .0005; ****, P ≤ .0001

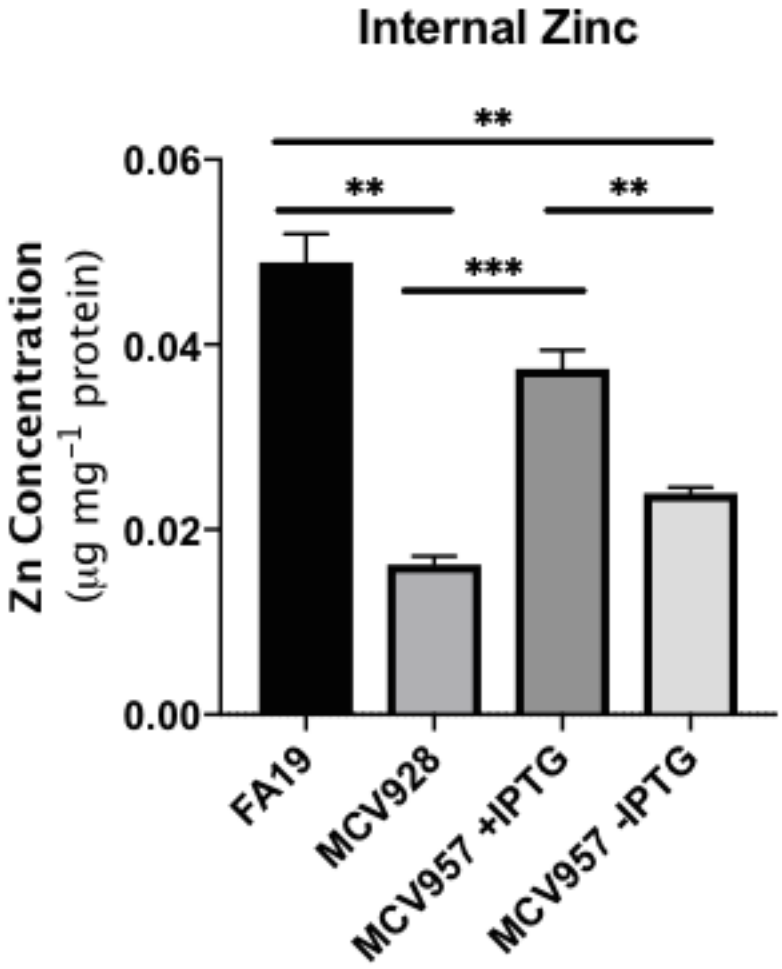
Internal Zinc
**
**
**
***
0.06
0.04
0.02
0.00
Zn Concentration
(μg mg−1 protein)
FA19
MCV928
MCV957 +IPTG
MCV957 -IPTG

IX. S100A7 Zinc Chelation is Essential for Utilization by TdfJ

Lastly, as concerns the TdfJ/S100A7 interaction, we were interested to see if S100A7 binding zinc *specifically* is what allows growth support of the gonococcus. Since the S100 proteins are capable of binding more than just zinc (56), we tested whether other metals may play a role in S100A7-mediated growth. We grew strain FA19 in zinc-depleted CDM supplemented with a double His-Asn (H87N, H91N) mutant S100A7 (Zn KO S100A7) that is unable to bind zinc. This mutant had been previously mixed with $ZnSO_4$ for sufficient time to allow zinc loading in the wild-type protein, before being dialyzed against buffer containing Chelex-100 to remove unbound metals. The mutant S100A7 showed no ability to support gonococcal growth, and was statistically indistinguishable from samples treated with no zinc, suggesting zinc presence in S100A7 is key for its role in gonococcal growth. (Fig 18).

X. *N. gonorrhoeae* Depends on the High-Affinity Zinc Uptake System ZnuABC to Utilize S100A7 and the Other S100s.

ZnuABC, the high affinity zinc transporter, has been a consistent factor present in Gram-negative bacteria that employ TdTs to acquire metals (69, 84). We wanted to assess whether this was true for the S100A7/TdfJ interaction and for the other S100s as well. We utilized In-Fusion® cloning to generate a *znuA* null mutant, MCV951, in the FA19 background. The schematic of this mutant's construction is outlined in figure 3. MCV951 is not a viable strain under standard growth conditions, and as such its growth must be supplemented at least with 5mM D-mannitol, and ideally with 25µM each of zinc and manganese if experiments allow. The

Figure 18. Mutant S100A7 unable to bind zinc is deficient in TdfJ-dependent growth support. Both wild-type S100A7 and mutant S100A7 incapable of binding zinc were mixed with $ZnSO_4$ at a 2:1 molar ratio and incubated with end-over-end mixing for 18h to allow any zinc loading to occur. After this, both mixtures were dialyzed against Chelex-100-treated dialysis buffer to remove any unbound ions before being utilized in growth premix. Strain FA19 was grown in Zn-restricted supplemented with premix containing either wild-type or mutant S100A7, with OD_{600} readings taken every 2h for 6h total. The graph demonstrates means and SD for n=3 independent experiments. A 2-way repeated measures ANOVA with Tukey's correction was performed for all means, with significance at 6h shown. *, P ≤. 05; **, P ≤ .005; ***, P ≤ .0005; ****, P ≤ .0001

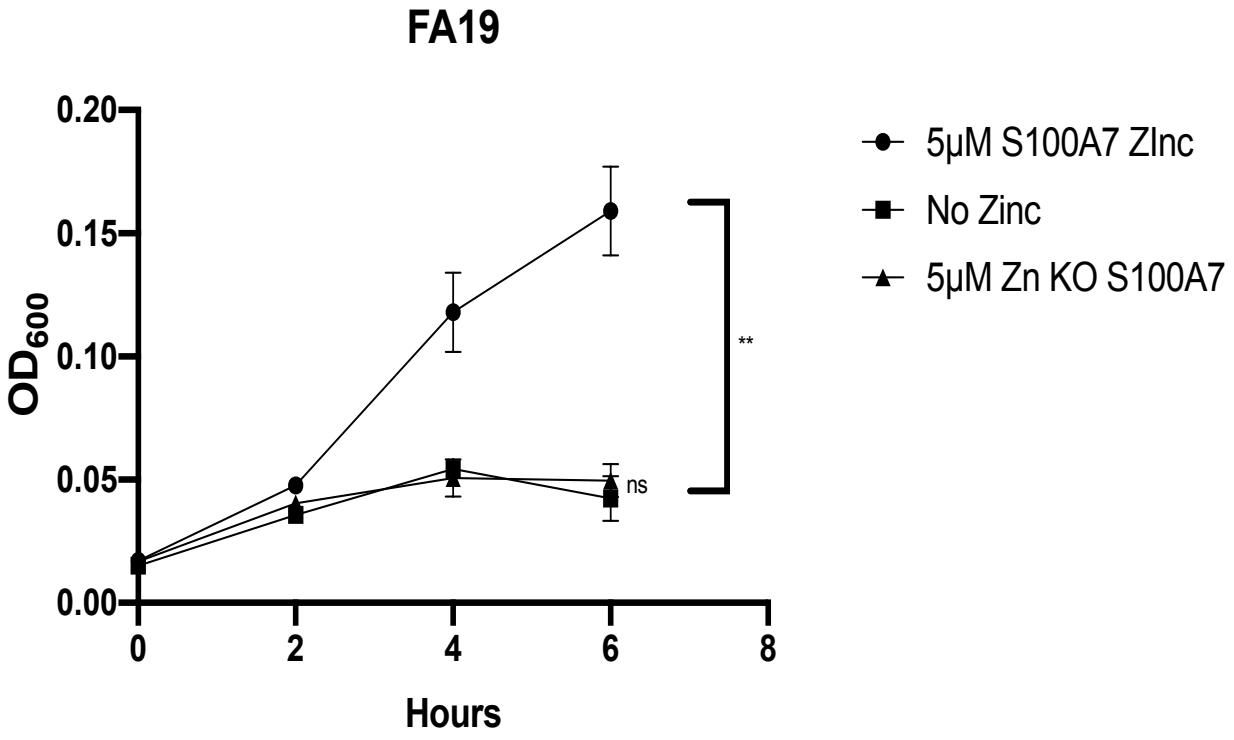
FA19
0.20
0.15
0.10
0.05
0.00
OD600
0
2
4
6
8
Hours
**
ns
5μM S100A7 ZInc
No Zinc
5μM Zn KO S100A7

generally nonviable nature of MCV951 is consistent with previous reports that suggest ZnuABC is required for helping bacteria overcome oxidative stress (85-87). In addition, we constructed an IPTG-inducible *znuA* complemented strain, MCV954. As MCV951 is particularly feeble, it is not a good candidate for transformation procedures, so construction of MCV954 took multiple intermediate steps (Fig. 4). We subcloned the full *znuA* gene from FA19 into pCR2.1 TOPO before transferring it to pVCU234. The resulting plasmid pVCU553 was used to transform FA19 to create a partial diploid of *znuA.* This strain then retroactively had its native *znuA* locus disrupted by the same methods used to create MCV951. We assumed there was a 50/50 chance that the ectopic locus and not the native locus would be disrupted, so we identified the correct genotype by Southern blotting, as shown in figure 19.

To assess the ability of MCV951 to utilize S100A7, we performed growth assays as described previously. When presented with S100A7 as a sole zinc source, MCV951 reached lower optical density than seen in samples treated with no zinc, and was significantly lower than samples given free zinc (Fig. 20). In addition to S100A7, we tested the other S100 proteins in the same manner. The same phenomenon was seen for each of the S100s in question except for S100A4, which was not investigated further (Fig. 21). These data suggest that a functional ZnuA is necessary for utilization of the S100s, and that those other than A7 are utilized in a Ton-independent manner. The mechanism for this is not clear and was not pursued in these studies. Finally, strain MCV954 was grown as described with and without IPTG to determine whether it could recover utilization of S100A7 (Fig. 22). The other S100s were not tested in this manner. When induced with IPTG, MCV954 recovered utilization of S100A7 and reached optical densities significantly higher than those seen in samples treated with free zinc.

Figure 19. Confirmation of MCV954 by Southern blotting. FA19, MCV951, MCV952, and MCV954 chromosomes were digested with ClaI and fully separated on a TBE-agarose gel before being transferred to nylon membranes by bidirectional capillary transfer. After transfer, DNA was UV crosslinked to the membrane and pre-hybridized with salmon sperm DNA. After pre-hybridization, membranes were hybridized with freshly denatured biotinylated PCR product of either *znuA* or the Ω morker. After washing, hybridized DNA was detected by probing with streptavidin conjugated to alkaline phosphatase.

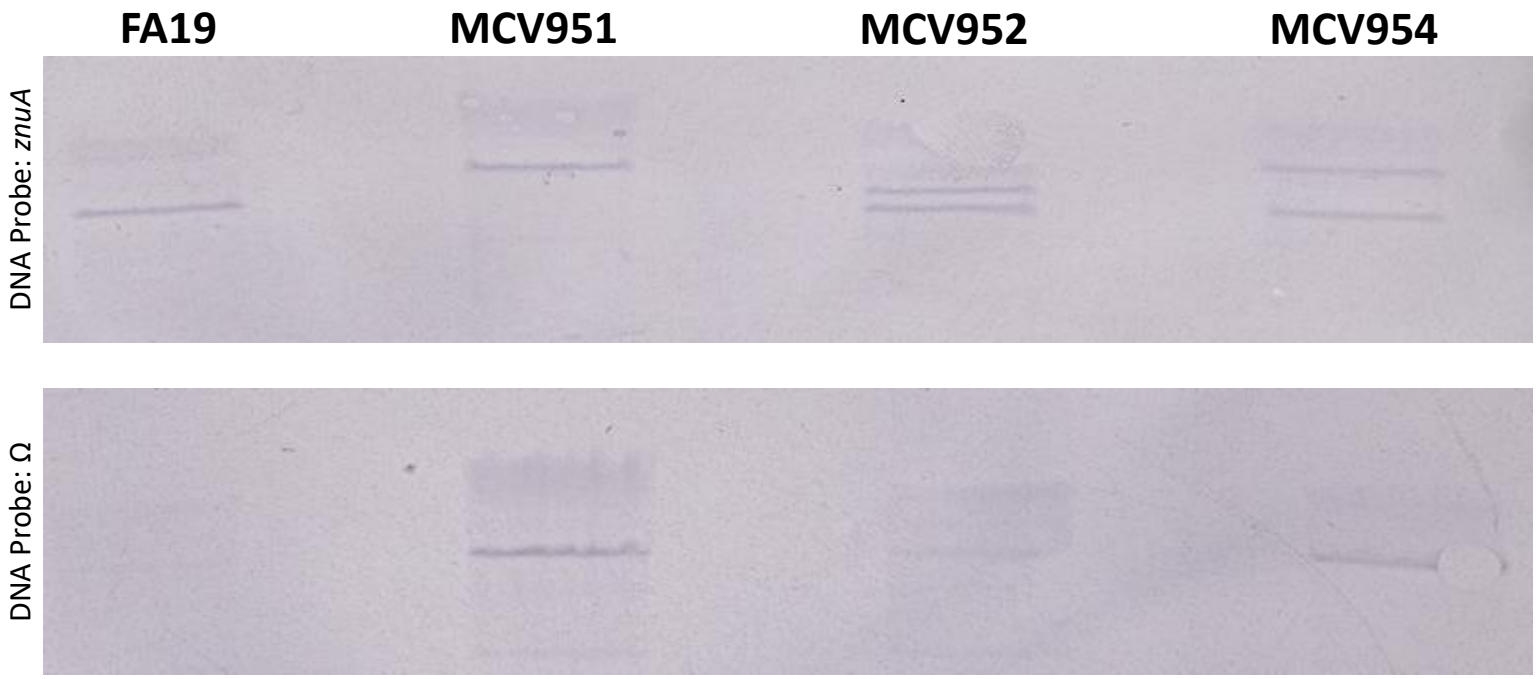
FA19
MCV951
MCV952
MCV954
DNA Probe: *znuA*
DNA Probe: Ω

Figure 20. A functional ZnuA is required for growth with S100A7. *N. gonorrhoeae* mutant strain MCV951 (*znuA*) was grown in Zn-limited conditions in defined media (CDM), which was supplemented with growth premix containing either $ZnSO_4$, S100A7, or no zinc. Growth was measured by OD_{600} readings every 2h for 6h total. Graph demonstrates means and SD for n=3 independent experiments. A 2-way repeated measures ANOVA with Tukey's correction was performed for all means, with significance at 6h shown. *, P ≤. 05; **, P ≤ .005; ***, P ≤ .0005; ****, P ≤ .0001

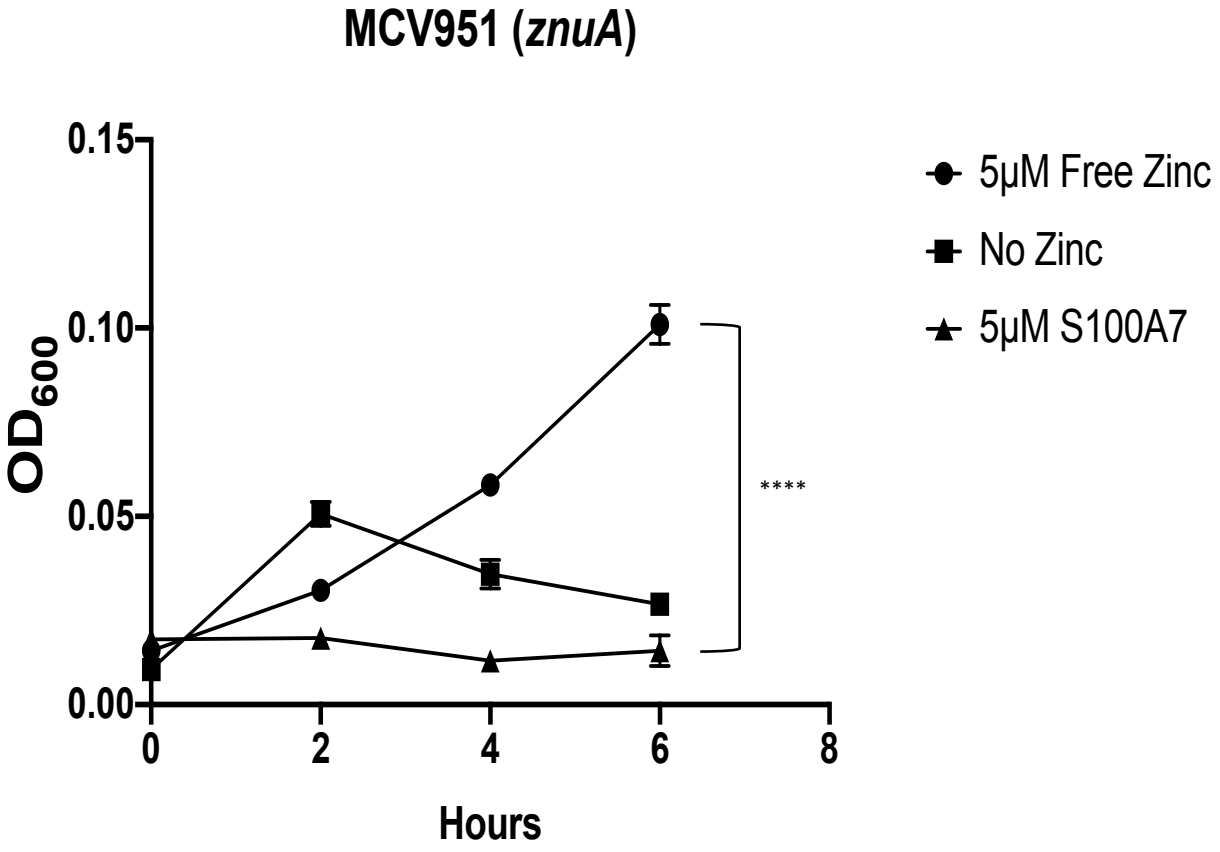
MCV951 (*znuA*)
0.15
0.10
0.05
0.00
OD_{600}
0
2
4
6
8
Hours
****
5μM Free Zinc
No Zinc
5μM S100A7

Figure 21. ZnuA is required for utilization of all S100 proteins except S100A4. *N. gonorrhoeae* mutant strain MCV951 (*znuA*) was grown in Zn-limited conditions in defined media (CDM), which was supplemented with growth premix containing either $ZnSO_4$, an S100 protein, or no zinc. Growth was measured by OD_{600} readings every 2h for 6h total.

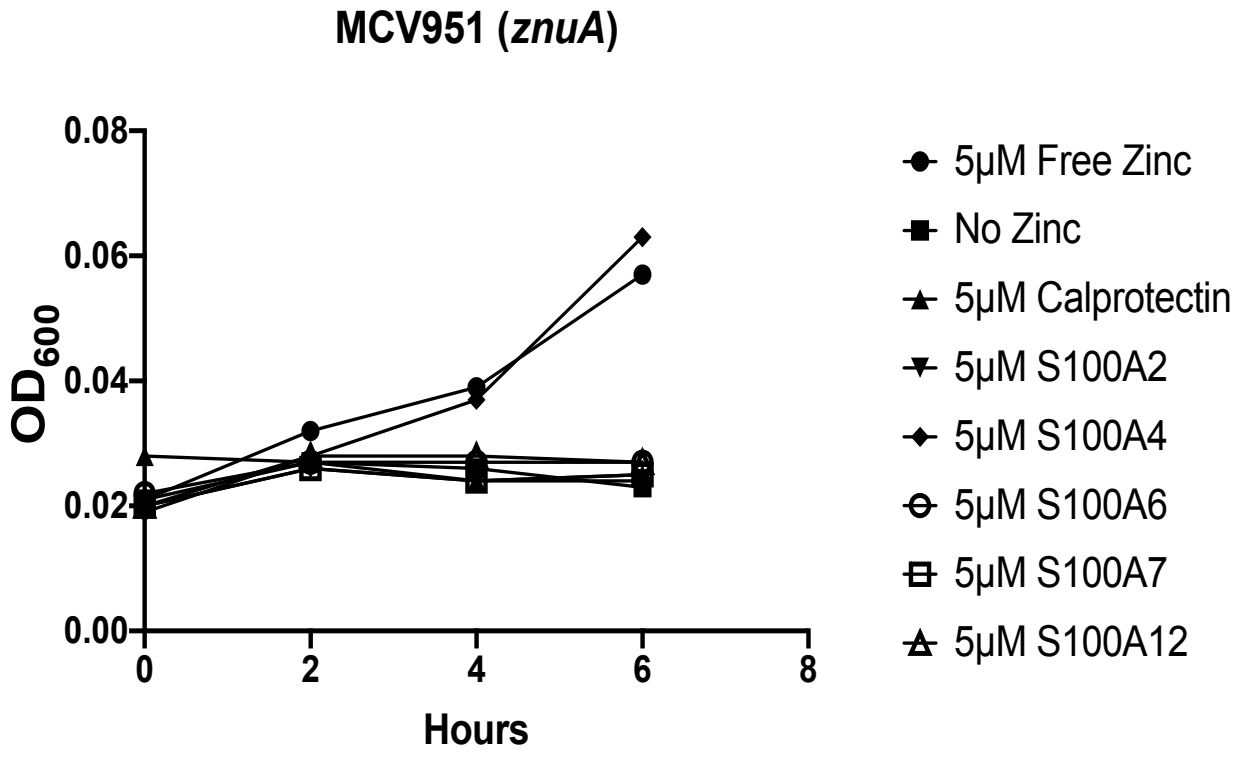
MCV951 (*znuA*)
0.08
0.06
0.04
0.02
0.00
OD_{600}
0
2
4
6
8
Hours
5μM Free Zinc
No Zinc
5μM Calprotectin
5μM S100A2
5μM S100A4
5μM S100A6
5μM S100A7
5μM S100A12

Figure 22. A functional ZnuA is required for growth with S100A7. *N. gonorrhoeae* mutant strain MCV954 (*znuA*^{C}) was grown in Zn-limited conditions in defined media (CDM), which was supplemented with growth premix containing either $ZnSO_4$, S100A7 with and without IPTG, or no zinc. Growth was measured by OD_{600} readings every 2h for 6h total. Graph demonstrates means and SD for n=3 independent experiments. A 2-way repeated measures ANOVA with Tukey's correction was performed for all means, with significance at 6h shown. *, P ≤. 05; **, P ≤ .005; ***, P ≤ .0005; ****, P ≤ .0001

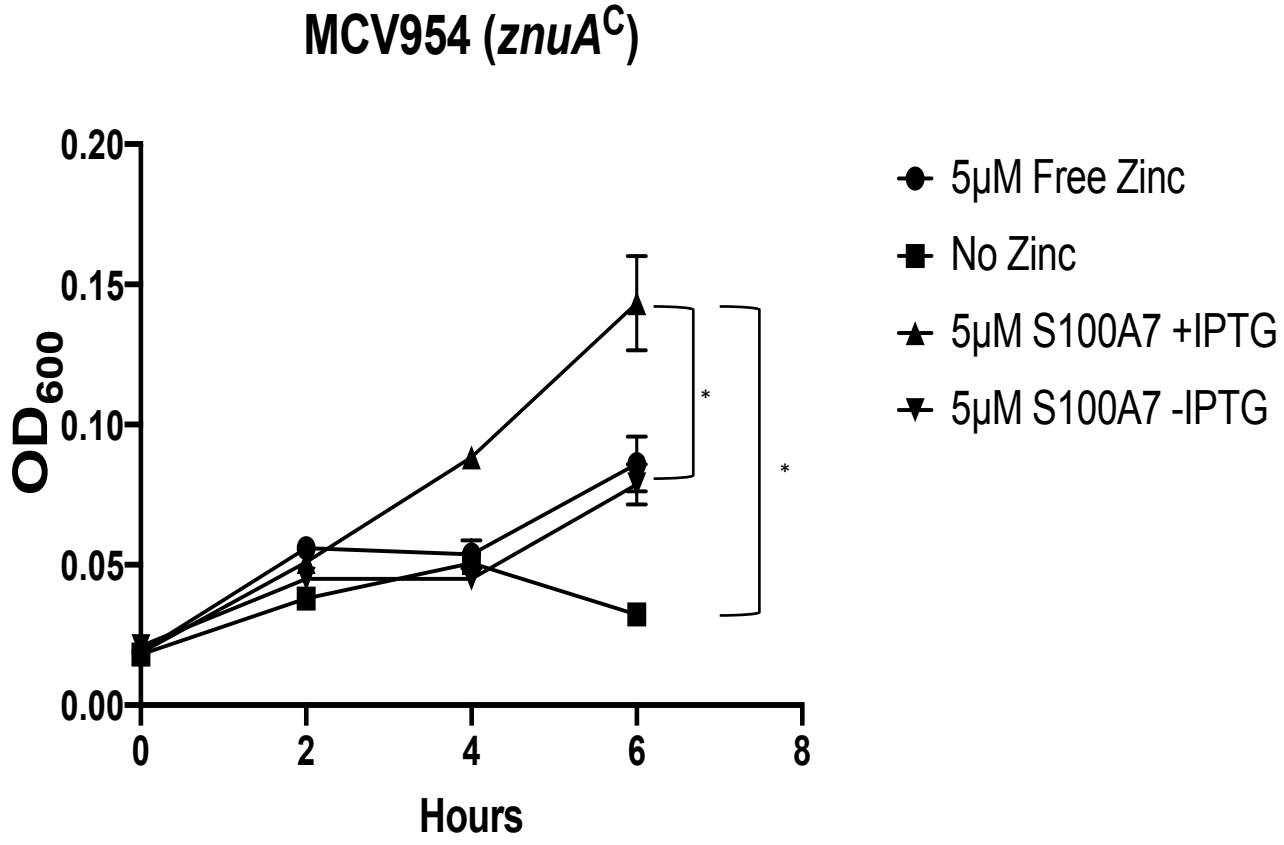
MCV954 (*znuA*^{C})
0.20
0.15
0.10
0.05
0.00
OD_{600}
0
2
4
6
8
Hours
*
*
5μM Free Zinc
No Zinc
5μM S100A7 +IPTG
5μM S100A7 -IPTG

Discussion

In the evolving arms race between host and pathogen, a prevalent theme has been nutritional immunity, which is the host's mechanism of restricting the availability of essential nutrients from invading pathogens, thus hindering their ability to establish infection. This is primarily accomplished by production of scavenging proteins that bind and sequester the nutrients in question, making them inaccessible (90). Many essential bacterial processes depend on transition metals such as zinc, iron, and manganese, making them key targets for this mechanism (88, 89). In response to nutritional immunity efforts, many pathogens have evolved the ability to produce and secrete siderophores, which are high-affinity compounds capable of out-competing host scavenging proteins and securing metal ions for use by the bacteria (91). Unlike most pathogens, however, *N. gonorrhoeae* does not produce siderophores, and is instead capable of overcoming nutritional immunity by non-traditional mechanisms. Rather than siderophores, *N. gonorrhoeae* utilizes an arsenal of outer-membrane proteins called TonB-dependent transporters to bind directly to host nutritional immunity factors and strip them of their nutritional cargo. Of the eight known gonococcal TdTs, four (TbpA, LbpA, HpuB, and FetA) participate in iron acquisition from transferrin, lactoferrin, hemoglobin, and xenosiderophores produced by other bacteria, respectively (34). Recently, it

has become clear that in addition to iron, the gonococcus has dedicated TdTs this are employed in zinc acquisition; TdfH binds to human Calprotectin, and TdfJ was previously shown to bind free zinc (43, 44). Upon consideration of the high level of conservation, both structural and functional, of the TdTs, we hypothesized that the uncharacterized TdTs may play an important role in nutrient acquisition for the gonococcus in the context of host nutritional immunity, especially for zinc uptake. Additionally, recent studies have shown these transporters to be promising candidates for vaccine development (92, 93).

In our attempts to further characterize the TdTs, we turned our attention to the S100 family of proteins. The S100s are EF hand calcium binding proteins that play many key roles in vertebrates, including but not limited to participating in nutritional immunity (65). The aforementioned Calprotectin has antimicrobial effects against numerous pathogens by sequestering zinc and manganese, and participates in neutrophil bactericidal activity via its presence in NETs (60, 61). Indeed, other members of the S100 family have demonstrated similar antimicrobial mechanisms. Like Calprotectin, S100A7 and S100A12, commonly referred to as psoriasin and calgranulin C, respectively, contribute to killing of *S. aureus, P. aeruginosa, S. flexneri, H. pylori*, and *C. albicans* by sequestering zinc (65, 76, 94-99). While antimicrobial activity is not reported for all of the S100s, metal binding is a constant, so we looked beyond just the three proteins described above. In these studies, we found that when loaded with zinc, the S100 family proteins were capable of serving as a zinc source for *N. gonorrhoeae* in defined media, suggesting that the pathogen is able to co-opt these proteins which, in many cases are antimicrobial.

Having established that these proteins were indeed sufficient zinc sources, and knowing that TdfH binds Calprotectin, we decided to screen the other Tdfs (TdfF, TdfG, TdfJ) as potential receptors for the S100s in question. These experiments revealed that in the absence of TdfJ, growth was not supported by S100A7, suggesting that these proteins may be interacting partners during gonococcal infection. In addition, we constructed an IPTG-inducible *tdfJ* complemented strain that, when induced, completely recovered the S100A7-zinc growth phenotype. We went on to show that S100A7 growth support depends on TonB, which aligns with the hypothesis that it is a partner for TdfJ, and in conjunction with data from our induced complement, suggests that a functional (TonB active) TdfJ is sufficient for *N. gonorrhoeae* to use S100A7 as a sole zinc source. It is important to note that the *tonB* mutant utilized in this study is not able to use transferrin as an iron source, which was the preferred source for our assay. To circumvent this, we replaced transferrin with $Fe(NO_3)_3$, which is not utilized as readily as transferrin, so overall bacterial growth was in general lower for these experiments. All other growth experiments leading up to this point were repeated with this replacement iron source and all growth patterns were recapitulated (data not shown). Of the S100 proteins queried in this study, only Calprotectin and S100A7 were unable to support growth in the absence of TonB, which is the expected result for Tdf ligands.

TdfJ acting as a zinc importer is not unexpected, as its meningococcal homologue ZnuD has been shown to bind extracellular zinc (44), and TdfJ is regulated by the Zur regulator (100) and has been shown to contribute to gonococcal growth in zinc-restricted conditions (101, 102). These results are corroborated by our own experiments pertaining to the regulation of *tdfJ* expression. Jean et al (43) showed that in gonococcal strain FA1090, TdfJ production was

repressed by zinc presence and induced by iron, but these metals were only considered individually and not in concert with each other. We expanded these studies to FA19 and assessed whether zinc absence and iron presence had a combined effect on TdfJ. We found that like FA1090, FA19 TdfJ is zinc repressed and iron induced, and that when both conditions are met, TdfJ production is maximal. These conditions were applied to all experiments requiring TdfJ production.

We next turned our attention towards asking whether TdfJ and S100A7 directly interacted with each other to facilitate the observed growth phenotype. Our data showed, via two approaches, that these two proteins directly bind to each other both when TdfJ is expressed on the cell surface and when purified. When gonococcal cultures were grown in conditions optimal for TdfJ production, both FA19 and the induced *tdfJ* complement, MCV957, were able to directly bind S100A7 in whole-cell solid-phase binding experiments. Gonococci lacking TdfJ on their surface generated no detectable binding, suggesting that a direct protein-protein interaction exists. Moreover, the growth conditions used are also ideal for production of the related zinc transporter TdfH, so this protein was present on the outer membrane as well. The lack of S100A7 binding to *tdfJ* mutant strains that still express a functional TdfH indicates that this interaction is indeed specific for TdfJ and not just TdTs in general. We considered the possibility that inactivating the *tdfJ* gene, which encodes a membrane-embedded protein, may have generated unexpected, unintended alterations to the outer membrane as a whole, and thus potentially confound binding experiments. To address this, we probed recombinant *E. coli* expressing either gonococcal TdfJ or containing an empty vector and found that TdfJ presence alone is sufficient for S100A7 binding, thus confirming their

interaction. In addition to whole-cell binding assays, we also utilized affinity pulldowns in an attempt to specifically elute TdfJ from an affinity matrix that had S100A7 conjugated to it. Only when passed over a matrix presenting S100A7 was recombinant TdfJ present in the specific eluate, and when another TdT, TdfF, was passed over this matrix, S100A7 did not bind. From these data, we conclude that S100A7 is the specific ligand for TdfJ and that they directly bind each other.

As an obligate human pathogen, *N. gonorrhoeae* utilizes many virulence factors that are restricted to the human host (83). Relevant TdT examples include TbpA exclusively binding human transferrin and TdfH only binding human Calprotectin. By utilizing mouse S100A7 (mS100A7) in whole-cell binding assays, we demonstrated that both gonococcal and recombinant TdfJ bind only to the human version of S100A7, and do not interact with the mouse version. While mouse S100A7 shares only 34% sequence identity with its human counterpart, its expression patterns, structure, and function are similar in both mice and humans (103, 104). Even when present at 10-fold molar excess, mS100A7 shows no ability to compete for binding. In identical growth experiments as performed previously, we showed also that when presented to the gonococcus as a zinc source, mS100A7 is unable to support bacterial growth, and indeed seems to directly hinder growth. We anticipate this is due to mouse S100A7 chelating the remaining free zinc from the growth medium, which is then unavailable to the pathogen. Taken together, these data show that TdfJ's interaction with S100A7 is specific to the human host, which agrees with previous reports on TdT/host interaction.

Finally, we moved our attention towards clarifying the fate of zinc in the TdfJ/S100A7 system. TdfH internalizes zinc from Calprotectin (43), but zinc internalization is not seen with its meningococcal homologue CbpA (102), so it was unclear which would be true for TdfJ. We utilized inductively coupled plasma optical emission spectrometry to quantify the amount of cellular zinc in gonococcal strains growth with S100A7 as a sole zinc source. We found that gonococci presenting a functional TdfJ accumulated significantly more internal zinc than strains not producing this protein, suggesting that the binding of S100A7 by TdfJ directly leads to zinc internalization, aligning with the activity of TdfH towards Calprotectin. To complement these data, we employed a mutant version of S100A7 in which two of the four zinc chelating histidine residues were mutagenized to asparagine, thus rendering the protein defective for zinc chelation. When this protein was incubated with same concentration of zinc as was present for saturation of wild-type S100A7 and subsequently used as a zinc source for *N. gonorrhoeae in vitro,* it showed significantly reduced growth support compared to the wild-type protein and was statistically indistinguishable from cultures grown with no zinc. These experiments demonstrate that the ability of S100A7 to bind zinc *specifically* is what allows it to support gonococcal growth, and that other transition metals seemingly do not play a role.

Having demonstrated that TdfJ utilizes S100A7 for the purpose of zinc internalization, we next wanted to elucidate how the zinc ions were passed from the periplasmic space across the gonococcal inner membrane and into the cytoplasm. To this end, we turned our attention to the high-affinity zinc transporter ZnuABC, which has been called MntABC elsewhere in the literature due to its ability to also serve as a manganese transporter (105). Many Gram-negative bacteria that utilize TdTs also produce ZnuABC (69, 84). We constructed a *znuA* null mutant and

an inducible *znuA* complemented strain for the purpose of utilizing growth assays to determine the contribution of ZnuABC to S100 utilization. We first screened the available S100 proteins for growth support in the *znuA* null mutant, and found that all S100s except S100A4 were defective for growth support in this mutant. We did not explore S100A4 further, so explanations for its behavior in growth assays are left to speculation. Keeping in mind that it did not show a statistically significant ability to support growth of a wild-type gonococcal strain when used as a zinc source, it is feasible that S100A4 is a poor zinc chelator, so changes in a gonococcal zinc uptake pathway are a poor way to characterize it; unchelated zinc from the initial protein loading step could support growth of both FA19 and MCV951. We repeated these growth experiments focusing on only S100A7 in order to highlight ZnuABC in the context of TdfJ, and confirmed that it no longer supports gonococcal growth in this mutant, suggesting that ZnuABC is indeed the method for zinc crossing the inner membrane. We further demonstrated that an induced *znuA* complement recovered the ability to utilize S100A7. From these data, we postulate a model wherein TdfJ binds S100A7 at the outer membrane and strips it of its zinc, which is passed into the periplasm and subsequently bound by ZnuA, which then uses ZnuBC to pass zinc into the cytoplasm.

In this report, we define a novel interaction between a gonococcal TdT (TdfJ) and the human zinc-binding protein S100A7, wherein TdfJ on the gonococcal surface directly binds S100A7 and utilizes if for zinc internalization, thus overcoming one type of host-mediated nutrient restriction. This interaction, unique to the human host, may provide a clear selective advantage to *N. gonorrhoeae* in the context of infection, especially at the mucosal epithelium, a biologically relevant niche for the gonococcus where S100A7 is enriched (95, 96). Moreover, we

show that other S100 proteins support gonococcal growth as a sole zinc source by an as-yet-unidentified manner. While the mechanism for this is not yet clear, TonB-independent siderophore-iron uptake has been observed (33, 79), so this is not unprecedented; ZnuA may extract zinc from the S100s assuming they are able to access the periplasm by non-TdT mechanisms. In light of these findings, we posit TdfJ as a promising vaccine target for this important pathogen. TdfJ is exposed on the bacterial surface and is not subject to the high-frequency phase and antigenic variation that has disqualified so many other surface structures from consideration. It has implications for importance in *in vivo* survival of the gonococcus by utilization of S100A7. Finally, TdfJ is ubiquitously found across the *Neisseria*, including the commensal strains from which gonococci and meningococci frequently acquire resistance factors, and which themselves may be opportunistic pathogens (106).

To summarize, we report a novel interaction between *N. gonorrhoeae* and its human host, which allows the gonococcus to overcome the innate immune mechanism of nutrient starvation. Considering the potential importance of this strategy for infection alongside TdfJ's presumed potential as a promising vaccine target, we anticipate further characterization of the TdfJ/S100A7 interaction in order to clarify the importance of TdTs as virulence factors for *N. gonorrhoeae.* Presumptive next steps may include characterizing the binding kinetics between S100A7 and TdfJ, or identifying key residues within the respective proteins which facilitate binding. Cash et al (112) showed that mutagenesis of key residues within TbpA prevented binding of transferrin, and reports have shown that mutant, nonbinding surface proteins in bacteria may have enhanced immunogenicity (93). With this in mind, a non-S100A7-binding mutant of TdfJ could be tested as a potential immunogen worthy of consideration as an

ingredient in a hypothetical gonococcal vaccine. Alternatively, therapeutic methods of combating active gonococcal infections by targeting TdTs in a manner that limits their ability to facilitate metal uptake may be explored as well. Finally, experiments must be performed in order to ascertain the conditions in which the gonococcus accesses S100A7 during infection, if it does so at all. Although S100A7 is produced in the mucosal epithelia, which is a biologically relevant environment as concerns gonococcal infection, we have not yet investigated the *in vivo* significance of the TdfJ/S100A7 interaction. It is anticipated that these experiments will be done in the near future.

Literature Cited

Literature Cited

1. Knapp, J. S. (1988). Historical perspectives and identification of Neisseria and related species. Clin. Microbiol. Rev., 1(4), 415.

2. Ma, M., Powell, D. A., Weyand, N. J., Rhodes, K. A., Rendón, M. A., Frelinger, J. A., & So, M. (2018). A Natural Mouse Model for Neisseria Colonization. Infection and Immunity, 86(5), 00839–17.

3. Johnson, A. (1983). The pathogenic potential of commensal species of Neisseria. J. Clin. Pathol., 36(2), 213.

4. CDC. 2018. Detailed STD Facts - Gonorrhea. Centers for Disease Control and Prevention.

5. Holmes KK, Counts GW, Beaty HN. Disseminated gonococcal infection. *Ann Intern Med*, 74, 979–993 (1971).

6. Edwards, J. L., & Apicella, M. A. (2004). The Molecular Mechanisms Used by Neisseria gonorrhoeae To Initiate Infection Differ between Men and Women. Clinical Microbiology Reviews, 17(4), 965–981.

7. Lambden, P. R., Heckels, J. E., James, L. T., & Watt, P. J. (1979). Variations in Surface Protein Composition Associated with Virulence Properties in Opacity Types of Neisseria gonorrhoeae. Microbiology, 114(2), 305–312.

8. van Putten, J. P. M., Duensing, T. D., & Carlson, J. (1998). Gonococcal Invasion of Epithelial Cells Driven by P.IA, a Bacterial Ion Channel with GTP Binding Properties. J. Exp. Med., 188(5), 941.

9. McCaw, S. E., Liao, E. H., & Gray-Owen, S. D. (2004). Engulfment of Neisseria gonorrhoeae: revealing distinct processes of bacterial entry by individual carcinoembryonic antigen-related cellular adhesion molecule family receptors. Infect. Immun., 72(5), 2742–2752.

10. Stolz, E., & Schuller, J. (1974). Gonococcal oro- and nasopharyngeal infection. Br. J. Vener. Dis., 50(2), 104.

11. Ngampasutadol, J., Ram, S., Gulati, S., Agarwal, S., Li, C., Visintin, A., ...Rice, P. A. (2008). Human factor H interacts selectively with Neisseria gonorrhoeae and results in species-specific complement evasion. J. Immunol., 180(5), 3426–3435.

12. CDC. 2006. Sexually Transmitted Disease Surveillance, 2005. U.S. Department of Health and Human Services. Centers for Disease Control and Prevention.

13. Miller, K. E. (2006). Diagnosis and treatment of Neisseria gonorrhoeae infections. Am. Fam. Physician, 73(10), 1779–1784.

14. Matejcek, A., & Goldman, R. D. (2013). Treatment and prevention of ophthalmia neonatorum. Can. Fam. Physician, 59(11), 1187.

15. WHO. 2018. Statistical Reports on Sexually Transmitted Infections (STIs)

16. CDC. 2015. 2014 Sexually transmitted disease surveillance. Department of Health and Human Services. Centers for Disease Control and Prevention.

17. Newman L, Rowley J, Vander Hoorn S, Saman Wijesooriya N, Unemo M, Low N, Stevens G, Gottlieb S, Kiarie J, Temmerman M. (2015). Global estimates of the prevalence and incidence of four curable sexually transmitted infections in 2012 based on systematic review and global reporting. PLOS One 10: e0143304.

18. CDC. 2018. Self-Study Gonorrhea Epidemiology. Centers for Disease Control and Prevention.

19. Fleming, D. T., & Wasserheit, J. N. (1999). From epidemiological synergy to public health policy and practice: the contribution of other sexually transmitted diseases to sexual transmission of HIV infection. Sex. Transm. Infect., 75(1), 3–17.

20. CDC. 2018. Gonorrhea Treatment.

21. WHO. 2015. Antimicrobial Resistance: Global Report on Surveillance.

22. Ohnishi, M., Golparian, D., Shimuta, K., Saika, T., Hoshina, S., Iwasaku, K., ...Unemo, M. (2011). Is Neisseria gonorrhoeae initiating a future era of untreatable gonorrhea? Detailed characterization of the first high-level ceftriaxone resistant strain. Antimicrob. Agents Chemother., 00325–11.

23. The Guardian. UK man has world-first case of super-strength gonorrhoea. (2018, March 28).

24. van der Woude, M. W., & Bäumler, A. J. (2004). Phase and Antigenic Variation in Bacteria. Clin. Microbiol. Rev., 17(3), 581.

25. Bergström, S., Robbins, K., Koomey, J. M., & Swanson, J. (1986). Piliation control mechanisms in Neisseria gonorrhoeae. PNAS, 83(11), 3890.

26. Boslego, J. W., Tramont, E. C., Chung, R. C., McChesney, D. G., Ciak, J., Sadoff, J. C., ...Bryan, J. R. (1991). Efficacy trial of a parenteral gonococcal pilus vaccine in men. Vaccine, 9(3), 154–162.

27. Stern, A., Brown, M., Nickel, P., & Meyer, T. F. (1986). Opacity genes in Neisseria gonorrhoeae: Control of phase and antigenic variation. Cell, 47(1), 61–71.

28. Schmidt, K. A., Schneider, H., Lindstrom, J. A., Boslego, J. W., Warren, R. A., Van de Verg, L., ...Griffiss, J. M. (2001). Experimental gonococcal urethritis and reinfection with homologous gonococci in male volunteers. Sex. Transm. Dis., 28(10), 555–564.

29. Murphy, G. L., Connell, T. D., Barritt, D. S., Koomey, M., & Cannon, J. G. (1989). Phase variation of gonococcal protein II: regulation of gene expression by slipped-strand mispairing of a repetitive DNA sequence. Cell, 56(4), 539–547.

30. Raymond, K. N., Dertz, E. A., & Kim, S. S. (2003). Enterobactin: An archetype for microbial iron transport. Proc. Natl. Acad. Sci. U.S.A., 100(7), 3584–3588.

31. Hood, M. I., & Skaar, E. P. (2012). Nutritional immunity: transition metals at the pathogen-host interface. Nat. Rev. Microbiol., 10(8), 525–537.

32. Skaar, E. P. (2010). The Battle for Iron between Bacterial Pathogens and Their Vertebrate Hosts. PLoS Pathog., 6(8), e1000949.

33. West, S. E., & Sparling, P. F. (1985). Response of Neisseria gonorrhoeae to iron limitation: alterations in expression of membrane proteins without apparent siderophore production. Infect. Immun., 47(2), 388.

34. Cornelissen, C. N., & Hollander, A. (2011). TonB-Dependent Transporters Expressed by Neisseria gonorrhoeae. Front. Microbiol., 2:117.

35. Wally, J., & Buchanan, S. K. (2007). A structural comparison of human serum transferrin and human lactoferrin. Biometals, 20(3-4), 249–262.

36. Noinaj, N., Guillier, M., Barnard, T. J., & Buchanan, S. K. (2010). TonB-dependent transporters: regulation, structure, and function. Annu. Rev. Microbiol., 64, 43–60.

37. Anderson, J. E., Sparling, P. F., & Cornelissen, C. N. (1994). Gonococcal transferrin-binding protein 2 facilitates but is not essential for transferrin utilization. J. Bacteriol., 176(11), 3162–3170.

38. Anderson, J. E., Hobbs, M. M., Biswas, G. D., & Sparling, P. F. (2003). Opposing selective forces for expression of the gonococcal lactoferrin receptor. Mol. Microbiol., 48(5), 1325–1337.

39. Chen, C. J., Sparling, P. F., Lewis, L. A., Dyer, D. W., & Elkins, C. (1996). Identification and purification of a hemoglobin-binding outer membrane protein from Neisseria gonorrhoeae. Infect. Immun., 64(12), 5008–5014.

40. Carson, S. D., Klebba, P. E., Newton, S. M., & Sparling, P. F. (1999). Ferric enterobactin binding and utilization by Neisseria gonorrhoeae. J. Bacteriol., 181(9), 2895–2901.

41. Hantke, K., Nicholson, G., Rabsch, W., & Winkelmann, G. (2003). Salmochelins, siderophores of Salmonella enterica and uropathogenic Escherichia coli strains, are recognized by the outer membrane receptor IroN. PNAS, 100(7), 3677–3682.

42. Capdevila, D. A., Wang, J., & Giedroc, D. P. (2016). Bacterial Strategies to Maintain Zinc Metallostasis at the Host-Pathogen Interface. J. Biol. Chem., 291(40), 20858–20868.

43. Jean, S., Juneau, R. A., Criss, A. K., & Cornelissen, C. N. (2016). Neisseria gonorrhoeae Evades Calprotectin-Mediated Nutritional Immunity and Survives Neutrophil Extracellular Traps by Production of TdfH. Infect. Immun., 84(10), 2982.

44. Stork, M., Bos, M. P., Jongerius, I., de Kok, N., Schilders, I., Weynants, V. E., ...Tommassen, J. (2010). An outer membrane receptor of Neisseria meningitidis involved in zinc acquisition with vaccine potential. PLoS Pathog., 6, e1000969.

45. Kumar, P., Sannigrahi, S., & Tzeng, Y.-L. (2012). The Neisseria meningitidis ZnuD zinc receptor contributes to interactions with epithelial cells and supports heme utilization when expressed in Escherichia coli. Infect. Immun., 80(2), 657–667.

46. Calmettes, C., Ing, C., Buckwalter, C. M., El Bakkouri, M., Chieh-Lin Lai, C., Pogoutse, A., ...Moraes, T. F. (2015). The molecular mechanism of Zinc acquisition by the neisserial outer-membrane transporter ZnuD. Nat. Commun., 6, 7996.

47. Hagen, T. A., & Cornelissen, C. N. (2006). Neisseria gonorrhoeae requires expression of TonB and the putative transporter TdfF to replicate within cervical epithelial cells. Mol. Microbiol., 62(4), 1144–1157.

48. Turner, P. C., Thomas, C. E., Stojiljkovic, I., Elkins, C., Kizel, G., Ala'Aldeen, D. A. A., & Sparling, P. F. (2001). Neisserial TonB-dependent outer-membrane proteins: detection, regulation and distribution of three putative candidates identified from the genome sequences. Microbiology, 147(5), 1277–1290.

49. Marri, P. R., Paniscus, M., Weyand, N. J., Rendón, M. A., Calton, C. M., Hernández, D. R., ...So, M. (2010). Genome sequencing reveals widespread virulence gene exchange among human Neisseria species. PLoS One, 5(7), e11835.

50. Chen, C. Y., Berish, S. A., Morse, S. A., & Mietzner, T. A. (1993). The ferric iron-binding protein of pathogenic Neisseria spp. functions as a periplasmic transport protein in iron acquisition from human transferrin. Mol. Microbiol., 10(2), 311–318.

51. Chen, C. Y., & Morse, S. A. (2001). Identification and characterization of a high-affinity zinc uptake system in Neisseria gonorrhoeae. FEMS Microbiol. Lett., 202(1), 67–71.

52. Lim, K. H. L., Jones, C. E., Hoven, R. N. v., Edwards, J. L., Falsetta, M. L., Apicella, M. A., ...McEwan, A. G. (2008). Metal Binding Specificity of the MntABC Permease of Neisseria gonorrhoeae and Its Influence on Bacterial Growth and Interaction with Cervical Epithelial Cells. Infection and Immunity, 76(8), 3569–3576.

53. Donato, R., Cannon, B. R., Sorci, G., Riuzzi, F., Hsu, K., Weber, D. J., & Geczy, C. L. (2013). Functions of S100 Proteins. Current molecular medicine, 13(1), 24.

54. Moews, P. C., & Kretsinger, R. H. (1975). Refinement of the structure of carp muscle calcium-binding parvalbumin by model building and difference Fourier analysis. J. Mol. Biol., 91(2), 201–225.

55. Yap, K. L., Ames, J. B., Swindells, M. B., & Ikura, M. (1999). Diversity of conformational states and changes within the EF-hand protein superfamily. Proteins, 37(3), 499–507.

56. Gilston, B. A., Skaar, E. P., & Chazin, W. J. (2016). Binding of transition metals to S100 proteins. Science China. Life sciences, 59(8), 792.

57. Baudier, J., Glasser, N., Haglid, K., & Gerard, D. (1984). Purification, characterization and ion binding properties of human brain S100b protein. BBA, 790(2), 164–173.

58. Goyette, J., & Geczy, C. L. (2011). Inflammation-associated S100 proteins: new mechanisms that regulate function. Amino Acids, 41(4), 821–842.

59. Brodersen, D. E., Nyborg, J., & Kjeldgaard, M. (1999). Zinc-binding site of an S100 protein revealed. Two crystal structures of Ca2+-bound human psoriasin (S100A7) in the Zn2+-loaded and Zn2+-free states. Biochemistry, 38(6), 1695–1704.

60. Kehl-Fie, T. E., Chitayat, S., Hood, M. I., Damo, S., Restrepo, N., Garcia, C., ...Skaar, E. P. (2011). Nutrient metal sequestration by calprotectin inhibits bacterial superoxide defense, enhancing neutrophil killing of Staphylococcus aureus. Cell Host Microbe, 10(2), 158–164.

61. Urban, C. F., Ermert, D., Schmid, M., Abu-Abed, U., Goosmann, C., Nacken, W., ...Zychlinsky, A. (2009). Neutrophil extracellular traps contain calprotectin, a cytosolic protein complex involved in host defense against Candida albicans. PLoS Pathog., 5(10), e1000639.

62. Gläser, R., Harder, J., Lange, H., Bartels, J., Christophers, E., & Schröder, J.-M. (2005). Antimicrobial psoriasin (S100A7) protects human skin from Escherichia coli infection. Nat. Immunol., 6(1), 57–64.

63. Moroz, O. V., Antson, A. A., Grist, S. J., Maitland, N. J., Dodson, G. G., Wilson, K. S., ...Bronstein, I. B. (2003). Structure of the human S100A12-copper complex: implications for host-parasite defence. Acta Crystallogr., Sect. D: Biol. Crystallogr., 59(Pt), 5.

64. Cornelissen, C. N. (2018). Subversion of nutritional immunity by the pathogenic Neisseriae. Pathogens and Disease, 76(1).

65. Zackular, J. P., Chazin, W. J., & Skaar, E. P. (2015). Nutritional Immunity: S100 Proteins at the Host-Pathogen Interface. J. Biol. Chem., 290(31), 18991.

66. Corbin BD, Seeley EH, Raab A, Feldmann J, Miller MR, Torres VJ, et al. Metal chelation and inhibition of bacterial growth in tissue abscesses. Science. 2008;319(5865):962-5.

67. Bianchi M, Niemiec MJ, Siler U, Urban CF, Reichenbach J. Restoration of anti-Aspergillus defense by neutrophil extracellular traps in human chronic granulomatous disease after gene therapy is calprotectin-dependent. J Allergy Clin Immunol. 2011;127(5):1243-52.e7.

68. Gaddy JA, Radin JN, Loh JT, Piazuelo MB, Kehl-Fie TE, Delgado AG, et al. The host protein calprotectin modulates the Helicobacter pylori cag type IV secretion system via zinc sequestration. PLoS Pathog. 2014;10(10):e1004450.

69. Hood MI, Mortensen BL, Moore JL, Zhang Y, Kehl-Fie TE, Sugitani N, et al. Identification of an Acinetobacter baumannii zinc acquisition system that facilitates

resistance to calprotectin-mediated zinc sequestration. PLoS Pathog. 2012;8(12):e1003068.

70. Sohnle PG, Hahn BL, Santhanagopalan V. Inhibition of Candida albicans growth by calprotectin in the absence of direct contact with the organisms. J Infect Dis. 1996;174(6):1369-72.

71. Liu JZ, Jellbauer S, Poe AJ, Ton V, Pesciaroli M, Kehl-Fie TE, et al. Zinc sequestration by the neutrophil protein calprotectin enhances Salmonella growth in the inflamed gut. Cell Host Microbe. 2012;11(3):227-39. doi: 10.1016/j.chom.2012.01.017.

72. Mueller, A., Schäfer, B. W., Ferrari, S., Weibel, M., Makek, M., Höchli, M., & Heizmann, C. W. (2005). The Calcium-binding Protein S100A2 Interacts with p53 and Modulates Its Transcriptional Activity. J. Biol. Chem., 280(32), 29186–29193.

73. Fei, F., Qu, J., Zhang, M., Li, Y., & Zhang, S. (2017). S100A4 in cancer progression and metastasis: A systematic review.

74. Nowotny, M., Spiechowicz, M., Jastrzebska, B., Filipek, A., Kitagawa, K., & Kuznicki, J. (2003). Calcium-regulated Interaction of Sgt1 with S100A6 (Calcyclin) and Other S100 Proteins. J. Biol. Chem., 278(29), 26923–26928.

75. Jansen, S., Podschun, R., Leib, S. L., Grötzinger, J., Oestern, S., Michalek, M., ...Brandenburg, L.-O. (2013). Expression and Function of Psoriasin (S100A7) and Koebnerisin (S100A15) in the Brain. Infection and Immunity, 81(5), 1788–1797.

76. Realegeno, S., Kelly-Scumpia, K. M., Dang, A. T., Lu, J., Teles, R., Liu, P. T., ...Modlin, R. L. (2016). S100A12 Is Part of the Antimicrobial Network against Mycobacterium leprae in Human Macrophages. PLoS Pathog., 12(6).

77. Yardan, T., Erenler, A. K., Baydin, A., Aydin, K., & Cokluk, C. (2011). Usefulness of S100B protein in neurological disorders. J. Pak. Med. Assoc., 61(3), 276–281.

78. Kenney CD, Cornelissen CN. Demonstration and characterization of a specific interaction between gonococcal transferrin binding protein A and TonB. J Bacteriol. 2002;184(22):6138-45.

79. Strange HR, Zola TA, Cornelissen CN. The fbpABC operon is required for Ton-independent utilization of xenosiderophores by Neisseria gonorrhoeae strain FA19. Infect Immun. 2011;79(1):267-78.

80. Chen, H., Bjerknes, M., Kumar, R., & Jay, E. (1994). Determination of the optimal aligned spacing between the Shine-Dalgarno sequence and the translation initiation codon of Escherichia coli mRNAs. Nucleic Acids Res., 22(23), 4953–4957.

81. Cooper, T. G., & Magasanik, B. (1974). Transcription of the lac Operon of Escherichia coli. J. Biol. Chem., 249(20), 6556–6561.

82. Ramsey, M. E., Hackett, K. T., Kotha, C., & Dillard, J. P. (2012). New Complementation Constructs for Inducible and Constitutive Gene Expression in Neisseria gonorrhoeae and Neisseria meningitidis. Appl. Environ. Microbiol., 78(9), 3068–3078.

83. Anderson MT, Seifert HS. Neisseria gonorrhoeae and humans perform an evolutionary LINE dance. Mob Genet Elements. 2011;1(1):85-7.

84. Amich J, Vicentefranqueira R, Mellado E, Ruiz-Carmuega A, Leal F, Calera JA. The ZrfC alkaline zinc transporter is required for Aspergillus fumigatus virulence and its growth in the presence of the Zn/Mn-chelating protein calprotectin. Cell Microbiol. 2014;16(4):548-64.

85. Seib KL, Wu HJ, Kidd SP, Apicella MA, Jennings MP, McEwan AG. Defenses against oxidative stress in Neisseria gonorrhoeae: a system tailored for a challenging environment. Microbiol Mol Biol Rev. 2006;70(2):344-61.

86. Tseng HJ, Srikhanta Y, McEwan AG, Jennings MP. Accumulation of manganese in Neisseria gonorrhoeae correlates with resistance to oxidative killing by superoxide anion and is independent of superoxide dismutase activity. Molecular microbiology. 2001;40(5):1175-86.

87. Wu HJ, Seib KL, Srikhanta YN, Kidd SP, Edwards JL, Maguire TL, et al. PerR controls Mn-dependent resistance to oxidative stress in Neisseria gonorrhoeae. Molecular microbiology. 2006;60(2):401-16.

88. Palmer LD, Skaar EP. Transition Metals and Virulence in Bacteria. Annu Rev Genet. 2016;50:67-91.

89. Lopez CA, Skaar EP. The Impact of Dietary Transition Metals on Host-Bacterial Interactions. Cell Host Microbe. 2018;23(6):737-48.

90. Hennigar, S. R., & McClung, J. P. (2016). Nutritional Immunity: Starving Pathogens of Trace Minerals. American Journal of Lifestyle Medicine, 10(3), 170–173.

91. Bullen JJ, Griffiths E (1999) Iron and infection: molecular, physiological and clinical aspects. New York: John Wiley and Sons.

92. Cash DR, Noinaj N, Buchanan SK, Cornelissen CN. Beyond the Crystal Structure: Insight into the Function and Vaccine Potential of TbpA Expressed by Neisseria gonorrhoeae. Infect Immun. 2015;83(11):4438-49.

93. Frandoloso R, Martínez-Martínez S, Calmettes C, Fegan J, Costa E, Curran D, et al. Nonbinding site-directed mutants of transferrin binding protein B exhibit enhanced immunogenicity and protective capabilities. Infect Immun. 2015;83(3):1030-8.

94. Madsen P, Rasmussen HH, Leffers H, Honoré B, Dejgaard K, Olsen E, et al. Molecular cloning, occurrence, and expression of a novel partially secreted protein "psoriasin" that is highly up-regulated in psoriatic skin. J Invest Dermatol. 1991;97(4):701-12.

95. Meyer JE, Harder J, Sipos B, Maune S, Klöppel G, Bartels J, et al. Psoriasin (S100A7) is a principal antimicrobial peptide of the human tongue. Mucosal Immunol. 2008;1(3):239-43.

96. Mildner M, Stichenwirth M, Abtin A, Eckhart L, Sam C, Gläser R, et al. Psoriasin (S100A7) is a major Escherichia coli-cidal factor of the female genital tract. Mucosal Immunol. 2010;3(6):602-9.

97. Gläser R, Harder J, Lange H, Bartels J, Christophers E, Schröder JM. Antimicrobial psoriasin (S100A7) protects human skin from Escherichia coli infection. Nat Immunol. 2005;6(1):57-64.

98. Andresen E, Lange C, Strodthoff D, Goldmann T, Fischer N, Sahly H, et al. S100A7/psoriasin expression in the human lung: unchanged in patients with COPD, but upregulated upon positive S. aureus detection. BMC Pulm Med. 2011;11:10.

99. Realegeno S, Kelly-Scumpia KM, Dang AT, Lu J, Teles R, Liu PT, et al. S100A12 Is Part of the Antimicrobial Network against Mycobacterium leprae in Human Macrophages. PLoS Pathog. 2016;12(6):e1005705.

100. Pawlik MC, Hubert K, Joseph B, Claus H, Schoen C, Vogel U. The zinc-responsive regulon of Neisseria meningitidis comprises 17 genes under control of a Zur element. J Bacteriol. 2012;194(23):6594-603.

101. Stork M, Bos MP, Jongerius I, de Kok N, Schilders I, Weynants VE, et al. An outer membrane receptor of Neisseria meningitidis involved in zinc acquisition with vaccine potential. PLoS Pathog. 2010;6:e1000969.

102. Stork M, Grijpstra J, Bos MP, Mañas Torres C, Devos N, Poolman JT, et al. Zinc piracy as a mechanism of Neisseria meningitidis for evasion of nutritional immunity. PLoS Pathog. 2013;9(10):e1003733.

103. Webb M, Emberley ED, Lizardo M, Alowami S, Qing G, Alfia'ar A, et al. Expression analysis of the mouse S100A7/psoriasin gene in skin inflammation and mammary tumorigenesis. BMC Cancer. 2005;5:17.

104. Wolf R, Voscopoulos CJ, FitzGerald PC, Goldsmith P, Cataisson C, Gunsior M, et al. The mouse S100A15 ortholog parallels genomic organization, structure, gene expression, and protein-processing pattern of the human S100A7/A15 subfamily during epidermal maturation. J Invest Dermatol. 2006;126(7):1600-8.

105. Coady, A., Xu, M., Phung, Q., Cheung, T. K., Bakalarski, C., Alexander, M. K., ...Nishiyama, M. (2015). The Staphylococcus aureus ABC-Type Manganese Transporter MntABC Is Critical for Reinitiation of Bacterial Replication Following Exposure to Phagocytic Oxidative Burst. PLoS One, 10(9).

106. Johnson AP. The pathogenic potential of commensal species of Neisseria. J Clin Pathol. 1983;36(2):213-23.

107. Mickelsen, P.A., and P. F. Sparling. 1982. Ability of *Neisseria gonorrhoeae, Neisseria meningitidis,* and commensal Neisseria species to obtain iron from transferrin and iron compounds. Infect. Immun. 33:555-564

108. Hagen, T.A. 2006. Mechanisms of Iron Acquisition Employed by *Neisseria gonorrhoeae* for Survival Within Cervical Epithelial Cells. Dissertation. Virginia Commonwealth University, Richmond, VA.

109. Oki, A.T. 2014. Characterization of the effects of iron on Neisseria gonorrhoeae surface protein modulation and host cell interactions. Dissertation. Virginia Commonwealth University, Richmond, VA.

110. Dickinson, M. K. (2014). Characterization of TonB-Dependent Metal Transporters within Neisseria gonorrhoeae. Dissertation. Virginia Commonwealth University, Richmond, VA.

111. Cash, D. R. (2016). DRUG AND VACCINE DEVELOPMENT FOR NEISSERIA GONORRHOEAEA. Dissertation. Virginia Commonwealth University, Richmond, VA.

112. Cash, D. R., Noinaj, N., Buchanan, S. K., & Cornelissen, C. N. (2015). Beyond the Crystal Structure: Insight into the Function and Vaccine Potential of TbpA Expressed by Neisseria gonorrhoeae. Infect. Immun., 83(11), 4438.

VITA

Stavros Andrew Maurakis was born in Danville, Virginia on the 12th of April, 1992. He graduated from Danville's George Washington High School, where he was very active with the marching band and soccer team, in 2010. Stavros received his Bachelor of Science degree in Microbiology and Immunology from Virginia Polytechnic Institute and State University in 2014. During his time there, he served as the vice-president of the Phi Sigma Biological Sciences Honor Society, and participated in various research programs on campus. After graduation, Stavros worked as a chemical research specialist for the Pet, Home, and Garden division of Spectrum Brands in Blacksburg, VA before beginning graduate study at Virginia Commonwealth University in fall of 2016. There, he joined the laboratory of Dr. Cynthia N. Cornelissen where he conducted the research for this thesis, and he will continue his formal education at the Ph.D. level in the immediate future. Stavros' favorite hobby is participating in competitive motorsports simulators, where he is active at the international level.

Publication:

Maurakis, S., Keller, K., Maxwell, C.N., Pereira, K., Chazin, W., Criss, A., Cornelissen, C. The Novel Interaction Between Neisseria gonorrhoeae TdfJ and Human S100A7 Allows Gonococci to Subvert Host Zinc Restriction. Under review as of this writing.